Investigating the impact of Haze, Clear and Cloudy Conditions on Nitrogen Dioxide retrieval from MAX-DOAS

By

Ahmad Iqbal

(00000203695)

A thesis submitted in partial fulfillment of the requirements for the degree of Master of Science in Environmental Science

Institute of Environmental Sciences and Engineering,

School of Civil and Environmental Engineering,

National University of Sciences and Technology

Islamabad, Pakistan

(2019)

THESIS ACCEPTANCE CERTIFICATE

It is certified that the contents and forms of the thesis entitled **"Investigating the impact of Haze, Clear and Cloudy conditions on Nitrogen Dioxide retrieval from MAX-DOAS"** submitted by **Mr. Ahmad Iqbal**, Registration No. **00000203695** has been found satisfactory for the requirements of the degree of Master of Science in Environmental Science.

Supervisor: _____
Dr. Fahim Khokhar
Professor
IESE, SCEE, NUST

Head of Department: _____
Dr. Muhammad Arshad
Associate Professor
IESE, SCEE, NUST

Principal: _____
Dr. Tariq Mahmood
SCEE, NUST

CERTIFICATE

It is certified that the contents and forms of the thesis entitled **"Investigating the impact of Haze, Clear and Cloudy conditions on Nitrogen Dioxide retrieval from MAX-DOAS"** submitted by Mr. Ahmad Iqbal has been found satisfactory for the requirements of the degree of Master of Science in Environmental Science.

Supervisor: _____
Dr. Fahim Khokhar
Professor
IESE, SCEE, NUST

Member:

_____
Dr. M. Zeeshan Ali Khan
Assistant Professor
IESE-SCEE, NUST

Member:

_____
Dr. Sher Jamal Khan
Professor
IESE-SCEE, NUST

I dedicate this thesis to my beloved parents and siblings who have been always a source of inspiration for me and stood beside me at every moment in my life.


بسم الله الرحمن الرحيم

ACKNOWLEDGEMENT

I would like to start with the name of **Almighty Allah**. All praise for Almighty "Allah″ who blessed me with complete code of life. All respect for **Holy Prophet Muhammad (Peace Be Upon Him)** whose life is pattern and ideal for us. And we have to follow him in all the paths of life.

I feel it as my foremost duty to express my due thanks to my supervisor **Professor Dr. Fahim Khokhar**, who provided me with all possible facilities and guidance for research. His keen interest and valuable suggestions are very precious and remained helpful throughout my research work. His dynamic supervision has been proved a useful guide for my research work. His special incredible guidance, sustained encouragement and sympathetic attitude during the period of my research enabled me to technically tackle all the problems during the course of study. The illustrious advices, valuable suggestions and inspiring attitude of **Dr. Zeeshan Ali Khan** and **Dr. Sher Jamal Khan** made it very easy for me to undertake this work throughout the course of this research work.

This acknowledgement would be incomplete if I do not pay my sincere and heartedly thanks to my cherished and loving parents for their sacrifices, prayers, and affections without which it would have been just a dream to achieve any goal. My sincerest thanks to all friends for their continuous support and encouragement throughout the research phase. Last but not the least I would like to thank all the laboratory staff at IESE for their help and cooperation.

Ahmad Iqbal

TABLE OF CONTENTS

LIST OF ABBREVIATIONS

AMF	Air Mass Factor
ArcGIS	Arc Geographic Information System
DOAS	Differential Optical Absorption Spectroscopy
DOASIS	Differential Optical Absorption Spectroscopy Intelligent System
DSCD	Differential Slant Column Densities
FTIR	Fourier Transform Infrared Spectrometry
FWHM	Full Width Half Maximum
HNO_3	Nitric Acid
JICA	Japan International Cooperation Agency
MAX-DOAS	Multi-axis Differential Optical Absorption Spectroscopy
NDIR	Non-Dispersive Infra-Red
NO	Nitric Oxide
NO_2	Nitrogen Dioxide
NO_2 SCD	Nitrogen Dioxide Slant Column Density
NO_2 VCD	Nitrogen Dioxide Vertical Column Density
NO_2^-	Nitrites
NO_3^-	Nitrates
NOx	Oxides of Nitrogen
O_3	Ozone
OMI	Ozone Monitoring Instrument
OSHA	Occupational Safety & Health Administration

Pak-EPA	Pakistan Environmental Protection Agency
Pak-NEQs	Pakistan National Environmental Quality Standards
PAN	Peroxy Acetyl Nitrile
PM	Particulate Matter
USEPA	United States Environmental Protection Agency
UTC	Coordinated Universal Time
UV	Ultra-Violet
VOCs	Volatile Organic Compounds
WHO	World Health Organization
WinDOAS	Windows Differential Optical Absorption Spectroscopy
ppb	Parts per Billion
RMS	Root Mean Square
OMI	Ozone Monitoring Instrument
VOCs	Volatile Organic Compounds
RMS	Root Mean Square

LIST OF TABLES

List of Figures

ABSTRACT

This study presents measurements of Nitrogen Dioxide (NO_2) column densities obtained by using Multi-axis Differential Optical Absorption Spectroscopy (MAX-DOAS) during different meteorological conditions such as haze, cloudy and clear sky. DOAS technique is a remote sensing method to retrieve concentration of various trace gases including novel Nitrogen Dioxide (NO_2). It is a criteria pollutant and is of paramount importance due to its role in atmospheric chemistry. It dissociates into other products in the presence of sunlight and is key component of various chemical reactions like ozone formation in troposphere. In this study comparison of different NO_2 dSCDs retrieval settings was made to find best NO_2 DOAS fit settings. Besides this, effect of hazy, clear and cloudy day on NO_2 concentration was explored. Furthermore, settings with different O_4 cross-sections were also compared to find the impact on best fit settings during cloudy condition. Comparison between results of different settings for NO_2 retrieval, reported in literature, and settings used for this study showed good correlation with $R^2 > 0.97$ ($R > 0.98$). NO_2 mean dSCD obtained during clear, cloudy and hazy conditions were 3.56E+16, 4.15E+16 and 4.01E+16, respectively. The results indicated that NO_2 concentration obtained on clear day was less than that of hazy and cloudy days due to larger photo-dissociation noted during clear condition. However, mean dSCDs in cloudy and hazy days were slightly higher as less or diffused sunlight was available in these conditions. This study further emphasized on validation of max DOAS observations with OMI satellite observations.

Chapter 1

1. INTRODUCTION

1.1. Background

Air Pollution is one of the most alarming environmental issues and is at the forefront of the critical challenges being faced by our societies. It is responsible for harmful effects on Human health as well as on ecosystem. Moreover, air pollution is also thought to be contributing to larger scale phenomenon like greenhouse effect and ozone layer depletion (Habeebullah, Munir, Morsy, & Mohammed, 2010).

Nitrogen Dioxide (NO_2), a criteria pollutant, formed as the consequence of fossil fuel consumption, includes sources like combustion processes, transportation and activities carried out in industries (Demirel, Özden, Döğeroğlu, & Gaga, 2014). Nitrogen oxides (NOx) is considered responsible for deteriorating environmental health in a number of ways. For example, NOx plays active role in destruction of Ozone layer, NOx as a whole is key ingredient of photochemical smog etc. (Salonen, Salthammer, & Morawska, 2019).

NO_2 concentration and impacts are increasing day by day which can be attributed to a number of factors like exponential growth of population during last few decades, more reliance on fossil fuel consumption, inefficient energy consumption etc. Besides, there are some other natural sources of NO2 like lightening and fire events that contributes to its emission (Frins et al., 2014).

NO_x is important as it plays a key role as a primary pollutant as well as secondary pollutant. High temperature achieved during fossil fuel combustion results in the formation of NO and consequently NO_2 in atmosphere, makes it a primary pollutant. However, NOx reaction with ozone is viewed as its role as secondary pollutant (Beard & Freas, 1994).

1.2. MAX-DOAS

MAX-DOAS (Multi-Axis Differential Optical Absorption Spectroscopy) is a new technique which is developed in last few decade. It is a ground-based remote sensing technique which measures scattered light from different slant or elevation angles to obtain the differential slant column densities (dSCD) of trace gases, present in the atmosphere. Its high sensitivity in atmosphere (specifically lower) makes this technique more reliable than other techniques used to retrieve profiles of atmospheric gases and aerosols. (Hönninger, Friedeburg, Platt, & Physics, 2004; Pikelnaya, Hurlock, Trick, & Stutz, 2007; Platt & Stutz, 2008; Theys et al., 2007; Wagner et al., 2004; Wittrock et al., 2004).

This technique has been used widely in different regions of world to acquire column information of Nitrogen Dioxide (NO_2) and various other pollutants (K. Chan et al., 2015; Clémer et al., 2010; Hendrick et al., 2014; Irie et al., 2008; X. Li et al., 2013; Ma et al., 2013; Vlemmix, Piters, Stammes, Wang, & Levelt, 2010; Wagner et al., 2011; Wittrock et al., 2004)

Figure 1.1 MAX-DOAS used in this study

1.3. Pakistan National Environmental Air Quality Standards

According to Pakistan National Environmental Quality Standards (Pak-NEQS) standards for certain pollutants are given for the ambient air:

Table 1.1.1 - NEQs for Ambient Air Quality

Pollutants	Time-weighted average	Concentrations in ambient air (µg/m3) Effective from 1st January 2012	Method of Measurement
Sulphur Dioxide (SO_2)	Annual Average	80	Ultraviolet Fluorescence Method
	24-hour Average	120	
Oxides of Nitrogen as (NO)	Annual Average	40	Gas Phase Chemiluminescence
	24-hour Average	40	
Oxides of Nitrogen as (NO_2)	Annual Average	40	Gas Phase Chemiluminescence
	24-hour Average	80 (42.5 ppbv)	
Ozone (O_3)	1-hour Average	130	Non Dispersion UV Absorption Method
Suspended Particulate Matter (SPM)	Annual Average	360	High Volume Sampling (Average Flow rate not less than 1.1 m^3/ minute)
	24-hour Average	500	
Respirable Particulate Matter (PM-10)	Annual Average	120	B Ray Absorption Method
	24-hour Average	250	
Respirable Particulate Matter (PM-2.5)	Annual Average	15	B Ray Absorption Method
	24-hour Average	35	
	1-hour Average	15	
	24-hour Average	1.5	
Carbon Monoxide (CO)	8-hours Average	5	NDIR
	1-hour Average	10	

Adopted from Ministry of Environment S.R.O. 1062(I)/2010.

1.4. Study Area

Islamabad, the capital of Pakistan is selected as site for this study. It is located at Latitude 33.349 N; Longitude 72.324 E, with elevation from sea level of about 450 meters (1827 ft.). Islamabad is mountainous region located in Pothohar Plateau. Its sub-tropical humid climate has two distinct seasons: Winter (October-March) and Summer (April-September)(Parekh et al., 2001). The instrument was mounted at the rooftop of Institute of Environmental Sciences

and Engineering (IESE), NUST. The lowest elevation angle used in this study was 2° as no high structure was present in the view field of telescope.

1.5. The Present Study

The primary objective of this study was to explore the behavior of atmospheric NO_2 during special weather conditions i.e. hazy, clear and cloudy days. Furthermore, it presents comparison of different NO_2 retrieval settings reported in literature. Very few studies have been conducted on effect of special weather conditions on NO_2 column densities. This study is significant as it also investigates the impact of different O_4 cross-sections on NO_2 retrieval settings. This study becomes significant because despite a lot of work has been done on retrieval of NO_2 column densities, very les work has been done on effect of different meteorological conditions on NO_2 concentration.

Chapter 2

2. LITERATURE REVIEW

2.1. Composition of Atmosphere

Our earth is enveloped by a number of gases, commonly known as air. It is divided in to four layers on the basis of the characteristics of each layer as:

2.1.1. Troposphere:

It is lowest layer of the atmosphere and its importance originates from the weather system that exists in this layer. It is also important as most the mass of atmosphere exists in this layer. The thickness of troposphere varies and is dependent on temperature and location. Its thickness ranges from 7 to 8 km at poles to 16 to 18km as equator. This variation is attributed to the rotation of earth as it tends to shift air masses towards equator. Besides temperature in always high at equator, as compared to poles, due to unequal distribution of insolation. With the increase in height, temperature decreases in this layer(Holton et al., 1995).

2.1.2. Stratosphere

The layer above troposphere, which extends up to 50km, is known as stratosphere. It is separated from troposphere by tropopause. It is second major layer of atmosphere. It is composed of 15% mass of the atmosphere and no weather exists here. It is layer where Ozone layer can be found which enhances the importance of this layer. Ozone layer blocks the harmful UV radiations that can cause serious problems like cancer and skin diseases. In other words, life would have been impossible to exist on this planet. In it, temperature increases with altitude. It is due to the heat which is produced as the result of ozone formation (Brasseur & Solomon, 2006; Holton et al., 1995).

2.1.3. Mesosphere

It is layer which is present above stratosphere and below thermosphere and is separated by these two by stratopause and mesopause, respectively. This layers height is up to 80 km. This layer is also important as it protects earth from all the meteors and asteroids that enter the atmosphere by burning them (due to friction)(Roble, Experiment, & Theory, 1995). The temperature decreases with increasing altitude in this layer.

2.1.4. Thermosphere

Thermosphere is layer which is immediately above the mesosphere and extends from 85km to 600km. It is layer where our telecommunication satellites work and is responsible for telecommunication on earth. Here, temperature increases with altitude because this layer is largely influenced by solar activity. In it, UV radiations results into creations of ions by photoionization of molecules(Lübken, 1999).

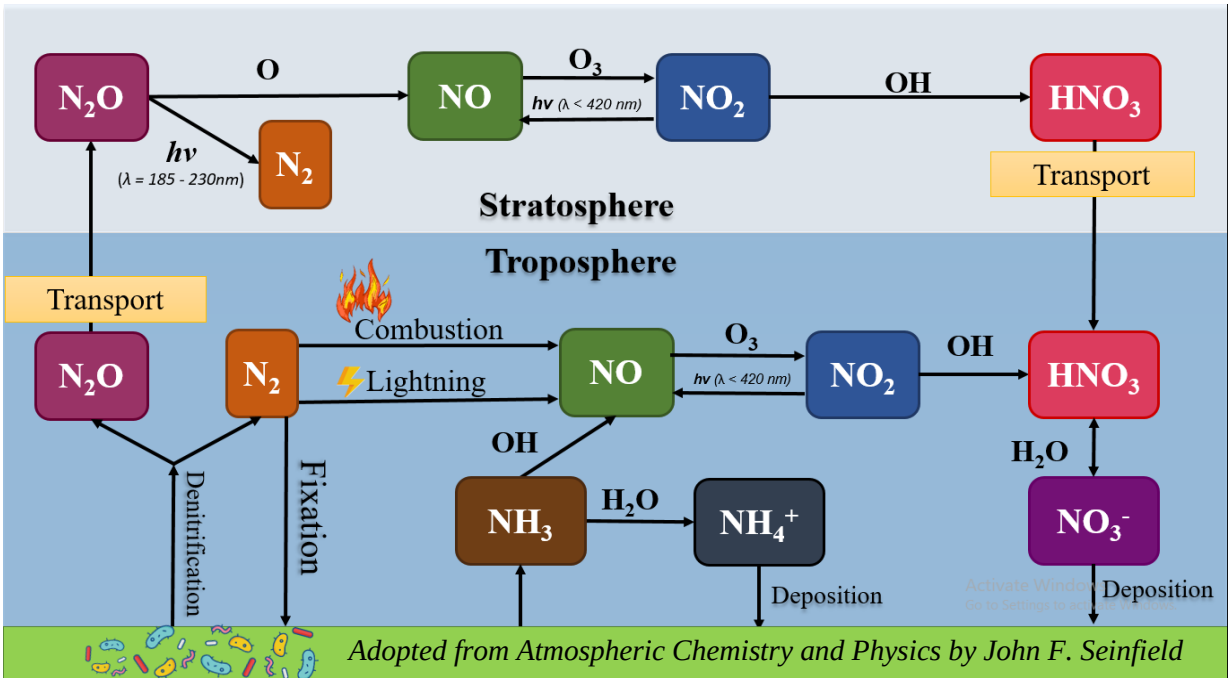

Figure 2.1 - Atmospheric Chemistry of NO2 in Troposphere and Stratosphere

2.2. Air Pollution

Air pollution is mainly excess of anything in air which alters the natural processes and affects the environment adversely. Natural and anthropogenic activities result in the release of various pollutants in environment that not only disturb the natural cycles but also cause adverse effects on human health. Gaseous pollutants such as NO_2 (Beelen et al., 2013), Ozone (Akimoto, 2003; Brook et al., 2002; Finlayson-Pitts & Pitts, 1997), Particulate Matter (PM_{10} and $PM_{2.5}$) (Dockery & Pope, 1994; Pope III et al., 2002; Pope III, Dockery, & association, 2006; Seaton, Godden, MacNee, & Donaldson, 1995), differ in composition, chemical activities and reactions, spatial and temporal distributions, and break down time. Exposure of such pollutants result in serious health effects. It ranges from causing cancer(Pope III et al., 2002) to respiratory disorders. Recent year studies have linked the air pollution with increased mortality(Bang, Nguyen, Vu, Hien, & Assessment, 2018; Dockery et al., 1993) and reduced life expectancy(Pope III, Ezzati, & Dockery, 2009). Persistent Organic Pollutants (POPs) and heavy are another categories of air pollutants that are considered as toxic due their longer disintegration time in environment. Their persistence is root cause of their toxicity. POPs when enter in food chain, they start cumulating in organisms. This accumulation may cross the toxic level and cause toxicity in organism. This process is called bioaccumulation (Schecter, Birnbaum, Ryan, & Constable, 2006).

2.3. A major criteria Pollutant: NO_2 (Nitrogen Dioxide)

Criteria pollutants are a set of pollutants that were first highlighted by United States Environment Protection Agency for the need of regulation because of their hazardous effects on human and environment in the form of acid rain, smog and other health related issues. Today, these are used to identify the quality of air. Nitrogen Dioxide (NO_2) is a pungent smell irritating gas. Its characteristic brown color is due to its ability to absorb light. It can be seen occasionally, as a brown haze, over major cities. It is a major criteria pollutant that has not been

in control since the beginning. It is so because of diversity in its sources i.e. automobile emissions, power-stations, factories and industries, etc. With rapid growth in population, during last few years, an upsurge of automobiles has been observed, which is considered as major air pollution contributor worldwide (Han & Naeher, 2006). Pakistan National Environmental Quality Standard, 2010 has suggested 80 μg/m3 of NO_2 as a limit for prevention of sensory irritation in population, for 24 hours. NO_2 exists in both, troposphere and stratosphere. It is an important trace gas which plays significant role in the chemistry of atmospheric in both spheres. In stratosphere, it plays key part in Ozone destruction cycle and transformation of Halogen Oxides (O-X) into much less reactive species. However, in troposphere, it is one of the significant precursors of ozone formation, Smog and acid rain. Besides, its contribution to radiative forcing also affects the chemistry of atmosphere.

2.4. Sources of NO_2

Nitrogen dioxide is mostly produces due the human activities. Its higher concentrations can be found in northern hemisphere, specifically mostly populated areas or in other words in urban centers. It is mainly due to fossil fuel burning, which provide conditions that favors the production of NOx in environment. According to recent studies, there is high uncertainty in emission sources of NO2 due to its shorter lifetime in atmosphere ranging from one to few hours. However transport sector is considered as major emission source of NO2 in atmosphere. Whereas air traffic in stratosphere results in its production in stratosphere (Badr & Probert, 1993). Natural sources includes biomass burning and agricultural practices. Moreover, emissions from the soil and microbial activities also contributes to NOx production by various processes like putrefaction affects the net NOx budget. Even thunderstorms result in the production of NOx in environment(Ibrahim, 2009).

Methane produced from soil when reacts with OH, it produces peroxy radicals (eq. 1 and 2). These radicals can oxidize nitric oxide into NO_2 (eq. 3)

$$CH_4 + OH \sim CH_3 + H_2O \quad \text{Eq. 1}$$

$$CH_3 + O_2 + CH_3O_2 \quad \text{Eq. 2}$$

$$CH_3O_2 + NO + NO_2 + CH_3O \quad \text{Eq. 3}$$

2.5. Measurement Techniques for NO_2

Since 19th Century, innovations have improved the instrumentation and methods being used to monitor ambient air quality. Today we have instrument with approximately 99% precision and accuracy. Several techniques are there that are being used to measure NO_2 concentrations. The applied techniques being used are as follows:

2.5.1. Chemiluminescence Methods

The Chemiluminescence technique for Nitrogen oxides measurement has been improved since its inception in 1970-80s (Drummond, Volz, & Ehhalt, 1985; Fontijn, Sabadell, & Ronco, 1970; Grosjean, Harrison, & technology, 1985; Pollack, Lerner, & Ryerson, 2010; Robinson, Bollinger, & Birks, 1999). Gaseous Nitric oxide reactions with ozone in excess is used, which is added in sample (air). Light of a specific wavelength is emitted from excited NO_2 production. The intensity of emission is measured either solid state detector or by photomultiplier tubes (PMT), and it is directly proportional to the NO concentration in the sample used. Nitrogen Dioxide measurement requires its regulated reduction to Nitric oxide either by photolytic conversion or by thermal decomposition, where NO_2 is derived by differential method.

2.5.2. Colorimetric Methods

In this method, colored species are produced when NO_2 is allowed to react with organic dye solutions. According to Beer Lambert's Law, optical absorbance of a chemical specie is directly proportional to the amount of that specie absorbed in solution or in other words, concentration of that species which is then measured by spectrophotometer. It is a sensitive

method as it is measured by spectrophotometer and dyes are needed to be analyzed immediately after the reaction as color complex forms in this process are quite instable. One major limitation of this method is unavailability of facilities in field and in remote areas. A number of analyzers have been designed on this principle (Chen et al., 2016; Riess & Standards, 1998) for NO_2 monitoring by the USEPA, Occupational Safety & Health Administration (OSHA) and National Institute for Occupational Safety and Health (NIOSH).

2.5.3. Electrochemical Sensor

Electrochemical sensors are cost effective and portable sensors that are being used to measure the ambient air quality. High sensitivity, cheaper price and longer sample retention time makes these sensors better among all other samplers. Its working principle is based on electrochemical reduction of nitrogen dioxide between electrodes, dipped in an electrolyte. NO_2 in sample diffuses into reaction chamber of cell where it is reduced at electrode. A potential difference is created due the produced electrons, which produces current directly proportional to the NO_2 concentration in sample. NO_2 concentration can me noted directly from the sensors. These samples are being used in order to find the NO_2 exposure in occupational assessments.

2.5.4. Passive Samplers

Since several years, passive sampling method is being use for monitoring air pollutants such as NO_2. In this technique, Plastic bags and membranes are deployed and employed at the site. By the process of diffusion, NO_2 is diffused in precise amount in the passive sampler which is the calculated through its partitioning co-efficient relative to the sampler.

2.5.5. Satellite Remote Sensing

Satellite observation have been considered and acknowledged widely as an important tool for the quantitative evaluation of distribution of atmospheric gases and composition (Beirle, Platt, Wenig, Wagner, & Physics, 2003; Burrows, Platt, & Borrell, 2011; Fioletov et al., 2013; Lee

et al., 2011; Lin, McElroy, & Physics, 2011; Martin, 2008; Richter, Burrows, Nüß, Granier, & Niemeier, 2005; Van Der A et al., 2008). In past few years, a lot of work has been done to study the emissions, sources, variation characteristics in different regions of the world, with satellite data e.g., for SO_2 (Boynard et al., 2014; Fioletov et al., 2013; C. Li et al., 2010), aerosols and NO_2 (Hilboll, Richter, Burrows, & Physics, 2013; Richter et al., 2005; Van Der A et al., 2006; S. Wang et al., 2012).

2.5.6. Spectroscopic Method (DOAS)

Differential Optical Absorption Spectroscopy (DOAS) is a reliable, sensitive and common technique to monitor atmospheric composition. It was first used by Plat and his coworkers in 1979. Its measurement of atmospheric trace gases is done by light source. In past, it has been applied to calculate the concentrations of many trace gases including, Hypobromite (BrO) by Sanders *et al.*, 1988 in stratosphere and by Hausmann and Platt, 1994 in troposphere, Nitrous acid (HONO) by Perner and Platt in1979 where by Platt in 1980, Formaldehyde (CHOCHO) by Volkamer *et al.* in 2005 and Nitrate (NO_3) by platt et al. in 1980. Besides, there are a number of other trace gases that absorb Ultra-Violet and Visible region that can be measured through this technique (PlattU, 2008), such as O_3, NO_2, SO_2, HCHO, OClO, H_2O and NH_3. It can measure several trace gases concurrently, which not only saves time but also allows analysis of different components of observed air masses. Generally, DOAS is performed using artificial light source, known as active DOAS technique and can be performed passively with natural light sources i.e. extraterrestrial light sources. Figure 2.2 shows simplified setup of DOAS. In it ***(***a) shows respective spectrum with absorption Structure of NO_2 (b) the light was convolved by the spectrograph and (c) shows the mapping by the detector.

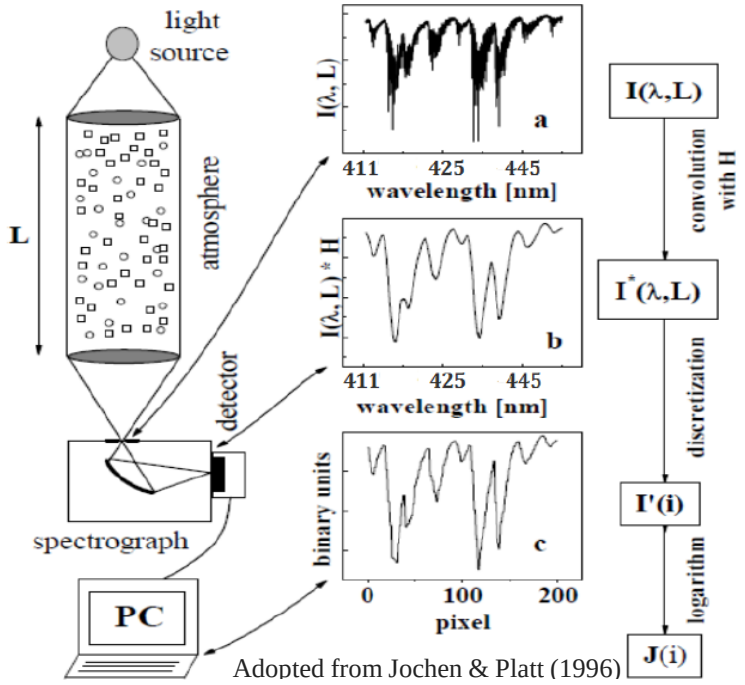

Figure 2.2 - The components of Simplified DOAS setup

2.6. NO_2 Chemistry in atmosphere

In troposphere, high temperature around 3000^oC, which can be achieved in total combustion engine and during lightening events, oxygen molecules breaks down into two oxygen atoms which are highly reactive in nature. These atoms reacts with nitrogen molecule and to produce NO. NO and NO_2 are referred to as NO_x due to their Intercomparison in atmosphere in the presence of Ozone (tropospheric). NO_2 rapidly breaks down into NO by UV radiations *(λ < 420 nm)* NO can be produced by reaction of hydroxyl ions with methane which is released from soil. This nitrogen dioxide can also settle down on the surface in the form of HNO_3 or acid rain(Guenther et al., 2000).

Microbial activity in soil produces N_2O which is comparatively stable. This N_2O when diffuse into stratosphere, it became unstable due to presence of shorter wavelength radiation (λ *=185-230 nm*), and breaks down into N_2 and O atom. This oxygen atom then again reacts with N_2 to form NO which converts into NO_2 in the presence of O_3.

During daytime, the interconversion of NO and NO_2 results into a Null cycle in which net production of the reaction is zero. Nitric oxide reacts with ozone molecule to produce nitrogen dioxide and oxygen molecule (eq.4)(Kreher et al., 2019).

$$NO + O_3 \rightarrow NO_2 + O_2 \qquad \text{Eq. 4}$$

Produced nitrogen dioxide breaks down in the presence of UV ($\lambda < 420$ nm) into nitric oxide and an oxygen atom (eq.5).

$$NO_2 + UV\ (\lambda < 420\ nm) \rightarrow NO + O\ (3P) \qquad \text{Eq. 5}$$

This oxygen atom reacts with oxygen molecule to form ozone again (eq. 6).

$$O\ (3P) + O_2 \rightarrow O_3 \qquad \text{Eq. 6}$$

However this cycle break down in the absence of UV radiations where nitrogen dioxide reacts with oxygen atom instead and produces oxygen molecule along with nitric oxide, and breaks null cycle (eq. 7).

$$NO_2 + O\ (3P) \rightarrow O_2 + NO \qquad \text{Eq. 7}$$

2.7. Impacts of Nitrogen Dioxide

Nitrogen Oxides affects the life, both aquatic and terrestrial. When Nitric oxide gets mix with ozone, it initiates the catalytic conversion of nitrogen dioxide into nitric oxide. This cycle continues naturally and maintains a balance. Due to anthropogenic activities, this cycle gets disturb. Due to the vehicular emissions and burning of fossil fuel in large quantities, habitat is adversely affected. Conditions turn worse when NO_2 is converted into nitric acid and settle down in the form of acid rain(Seangkiatiyuth, Surapipith, Tantrakarnapa, & Lothongkum, 2011). However, when NO_2 accumulate in urban areas, in certain meteorological conditions, pollution episodes are likely to happen like that of smog which not only affects lungs, eyes and skin of exposed humans but also affect the economic activities of the affected area.

NO and NO_2 are toxic in nature. These gases are mainly inhaled by humans from sources like industrial work and traffic. When NO_2 enters in the body, it starts accumulation and it turns into Nitric acid which affects the iron present in our blood thus denaturing the functionality of hemoglobin in our body. Due to low solubility of NO_2 in water, it can travel or reach deep into our lungs and can damage lungs. Short term exposure can cause irritation in breathing but ling term exposure can result loss of functioning of lungs tissue in extreme cases(Pandey, Kumar, & Devotta, 2005).

2.8. Recent Studies on NO_2 Pollution Monitoring

In recent years, optical methods are being used mainly to obtain NO_2 measurements in atmosphere. It is so because of several advantages of this method; for instance, high sensitivity, speedy measurements, measurement of more than one trace gas at a time and data retrieval at high resolution. (Lohberger, Hönninger, & Platt, 2004). MAX-DOAS, a type of Differential Optical Absorption Spectroscopy instrument, (Hönninger et al., 2004; Platt & Stutz, 2008; Vlemmix et al., 2015), has been used for retrieval of vertical densities of various trace gases (NO_2, O_3, CHOCHO, SO_2, BRO, IO ,HCHO and HONO)) (K. L. Chan et al., 2019; Coburn, Dix, Sinreich, & Volkamer, 2011; Hendrick et al., 2014; Khan, Khokhar, Shoaib, & Nawaz, 2018; Khokhar, Naveed, Butt, & Abbas, 2016; Kreher et al., 2019; Leser, Hönninger, & Platt, 2003; Y. Wang et al., 2017). This instrument has been reported to be used by applying to different platforms like ground-based, vehicle based, ship based and satellite based, for monitoring purpose (Dix, Koenig, & Volkamer, 2016; Halla et al., 2011; Lin et al., 2014; Peters et al., 2012; Shabbir, Khokhar, Shaiganfar, & Wagner, 2016; Shaiganfar et al., 2015).

To date, a lot of work has been done by using MAX-DOAS. Temporal pattern of tropospheric NO_2 VCDs was obtained from ground-based DOAS at Shangdianzi region of China and compared ground-based NO_2 VCDs measurements with OMI data (Cheng et al., 2019).

In another study, MAX-DOAS has been used for observation of tropospheric SO_2, NO_2 and HCHO in Hefei, Nanjing, and Shanghai (Yangtze River Delta area)(Tian et al., 2018). Even long term studies of over 5 years has been conducted by using Max-DOAS (K. Chan, Wiegner, Wenig, & Pöhler, 2018). Tropospheric By using MAX-DOAS, NO_2 measurements were obtained during the Shanghai World Expo 2010 (K. Chan et al., 2015).

Premuda and his coworkers exploited the NO_2 VCDs by using MAX-DOAS to conclude the degradation of coastal wooded zone from nearby city in Italy, attributed to atmospheric circulation and Coriolis Effect(Premuda et al., 2013). Takashime et al. observed the rapid air mass transport in Japan from the Eastern coast of the China using DOAS measurements and backward trajectory model. They have also highlighted that marine boundary layer affects the photodisintegration time of NO_2 in troposphere and allows the NO_2 to transport more than 700km towards site of the study. They further emphasized on the cross-boundary pollutant sources through this study(Takashima, Irie, Kanaya, & Akimoto, 2011).

Shaiganfar et al., 2011, monitored NO_2 concentration in New Dehli, India by using Car-based MAXDOAS in 2011. They have correlated the nitrogen dioxide concentrations with traffic load and other sources. Moreover, the observations were also validated using satellite data.

2.9. NO_2 Pollution Monitoring in Pakistan

In Pakistan, transportation, power and industrial sectors accounts for more than 70% of the NO_2 pollution. During the time period of 1995-2005, 33% increase in motor vehicles annually has been reported. This increase has affected the ambient air quality badly as the result of which, major cities like that of Lahore are experiencing episodes of Smog in winter.

Criteria pollutants has been monitored in three major cities by Pakistan Environmental Protection Agency and Japan International Cooperation Agency (JICA) in 2000. Various trace gases like Nitrogen oxides (NO_x), Sulphur Dioxide (SO_2) and Ozone (O_3), were monitored in

this study. High level NO_x concentrations were attributed to traffic congestion. However, Lahore was found to be most polluted among all.

Car-based MAX-DOAS has been used by Ali et al, to monitor ambient air quality along different cross sections of National highway 5 in Pakistan. They have measured various criteria pollutants including CO, SO_2, NO_x, PM and Noise levels, by using different techniques. It was observed that NO_2 concentration increased while moving towards Lahore from Gujranwala, along NH5. NO_2 levels in Lahore were found to be highest (Ali, Athar, & Assessment, 2008).

NO_2 pollution level in different areas of twin cities i.e. Rawalpindi and Islamabad were investigated by Zafar et al., 2012. Study was conducted in two parts on the basis of season. First phase was carried out in winter whereas second one in spring. Industrial activities and traffic congestion were correlated with NO_2 pollution level in this study (Zafar, Ahmad, Syed, & Ali, 2012).

Jahangir and his coworker's study focused mainly on monitoring NO_2 pollution level near hospitals in twin cities. They found higher NO_2 concentration near hospitals situated on the roads, mainly due to traffic congestion (Jahangir, Ahmad, Aziz, Shah, & Science, 2013).

Besides, ongoing research on ambient air quality at National University of Science and Technology (NUST) have taken many initiative into account to monitor air quality using Mini MAX-DOAS. With mobile monitoring, NO_2 VCDs have been retrieved in twin cities. Point source monitoring for Glyoxal (CHOCHO), Ozone (O_3), Sulphur Dioxide (SO_2) and formaldehyde (HCHO) have also been done. Database of NO_2 VCDs from satellite observations using SCIAMACHY, OMI and GOME-2 data has also been established to investigate the temporal and spatial trends of NO_2 pollution in Pakistan. Trends showed that NO_2 concentration varies throughout the year, with highest concentration in winter and lowest in summer.

Chapter 3

3. INSTRUMENTION AND METHODOLOGY

3.1. Mini Max-DOAS Instrument:

In order to quantify the tropospheric trace gases, the MAX-DOAS uses different elevation angles, from 0 to 90°, to capture the scattered sunlight (Bobrowski, Hönninger, Galle, & Platt, 2003). MAX-DOAS can measure a number of trace gases, at a time, in visible and Ultra-Violet Spectral ranges and resultant less residual allows its use in even less polluted environment. It is a light weighted instrument with dimensions of 13cm×19cm×14cm. MAX-DOAS instrument used in this study contains a 40mm lens mounted at the front, coupled with spectrograph by fiber optics and electronic circuit. Czerny-Turner spectrometer (USB 2000+, Ocean Optics In.), having spectral resolution of 0.7nm, records the scattered light of absorption spectra between 320-460nm, whereas stepper motor, installed in it, is used to move the entire instrument to achieve desired elevation angle. Scattered light enters the instrument via lens which is tightly sealed to avoid any condensation of water vapors and prevent dust particles to damage the interior optics.

Working Principle:

Lambert-Beer law is working principle of the DOAS technique, which states that transmittance of light i.e. electromagnetic radiation, is directly proportional to the concentration of a substance present in the optical path.

$$I(\lambda)=Io\ (\lambda)\ e - \alpha LC \qquad \text{Eq. 8}$$

Here, “Io” means incident intensity whereas “I” is referred to as measured intensities. This technique depends upon the difference in wavelengths in observed and reference spectrum. Various trace gases can be obtained simultaneously within selected fitting interval. It takes specific cross sections into consideration and by using spectra of desired gases, differential

slant column densities (dSCDs) can be retrieved. DOAS technique is used especially for the retrieval of those trace gases which have short lifetime in atmosphere like that of NO_2.

3.2. Software used for Research Work:

The estimation and plotting of Nitrogen Dioxide VCD required use of various software as presented in Table 3.1:

Table 3.1 - Software used in this study

Sr. No.	Software	Purpose
1	Differential Optical Absorption Spectroscopy Intelligent System (DOASIS)	Operating Software for Max-DOAS and measurement of back scatter intensities
2	Windows Differential Optical Absorption Spectroscopy (WinDOAS)	For Convolution and Calibration
3	QDOAS	Analysis of UV-visible Spectra to retrieve dSCDs
4	Microsoft Excel (v 2013)	Mathematical Calculations for tropospheric VCD extraction and Graphical representations
5	ArcGIS (v 10.3.1)	Interpolation of satellite (OMI) data

3.2.1. Differential Optical Absorption Spectroscopy Intelligent System (DOASIS)

DOASIS is used to run the MAX-DOAS instrument for the acquisition of the spectra. It also performs other important functions like controlling the stepper motor, Setting Peltier temperature, adjusting integration time of each spectrum etc. A java script is used to run the DOASIS which includes all the commands for its functioning. It can also be used for the calculation of the ring spectrum, which is required for the analysis in QDOAS. Dark current and Offset can be measured from this software manually.

Dark current is small current that is monitored for photosensitive devices like spectrometer. For its measurement, large Tini (Exposure/integration time) and less number of scans are selected. Offset is the measurements recorded in “No photons” condition, in other words, it is

measured in dark conditions. However, a smaller integration time and high scans are used for measuring offset spectra as shown in Table 3.2.

Table 3.2 - Values usually used for Dark Current and Offset measurement

	Integration/Exposure time(milliseconds)	**Scan numbers**
Dark Current	3	10000
Offset	10000-20000	1

3.2.2. Windows Differential Optical Absorption Spectroscopy (WinDOAS)

Wavelength Calibration:

For wavelength calibration, WinDOAS (Windows Differential optical absorption spectroscopy) was used. Spectrum taken at noon was used for the calibration purpose (usually taken at 90^{o} of noon time/with least SZA). In calibration, the fit was applied between a measured and a convoluted spectrum. Meanwhile, wavelength of the solar spectrum was attributed to the individual detector's pixels (2048). The calibration fit is also known as "Kurucz-fit" because a solar spectrum measured by Kurucz is usually used as input which is further convoluted as per the spatial resolution of the mini MAX-DOAS used in the monitoring. The wavelength range was divided into several sub-windows (subwindows= 6) for analyzing the fits in each sub-window. For adjustment of spectrum shift between convoluted and measured spectra, "shift and squeeze" was also applied. Slit Function Parameter (SFP) specifies that the interpolation of the results of the individual sub-window were carried out using polynomial degree. Repeated twice the calibration process, reduces the residual. All measure spectra are evaluated in this study using the calibration file against a reference spectrum.

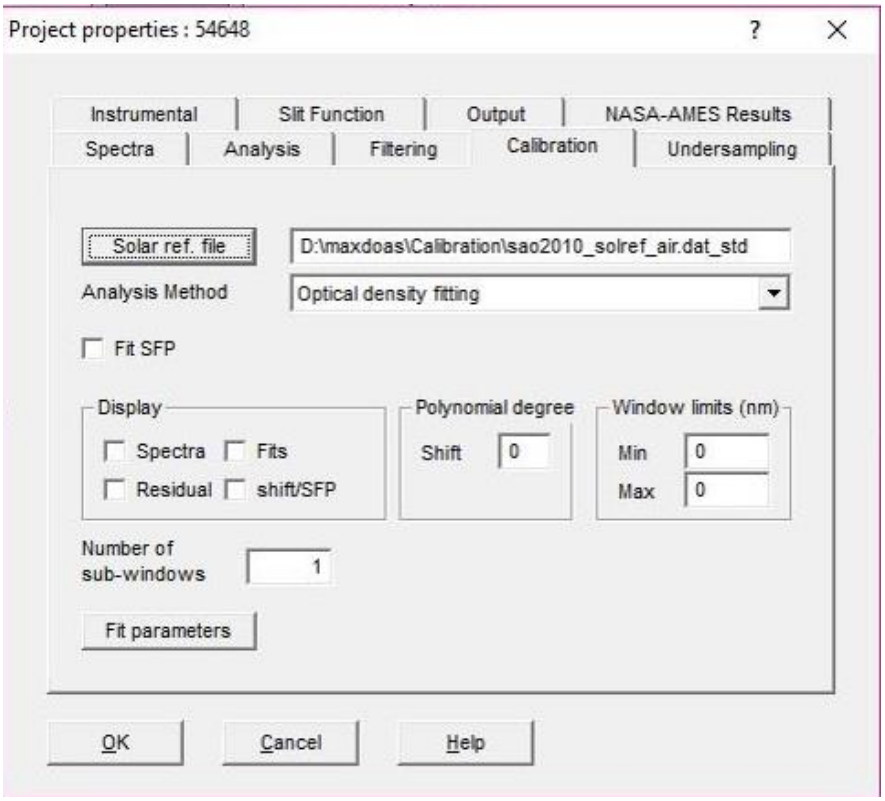

Figure 3.1 - Calibration window of WinDOAS

Wavelength Convolution:

This process was performed by using "Convolution tool" of WinDOAS software. It is a mathematical process which is important for wavelength processing operations.

NO_2 Analysis:

This is performed in QDOAS software. Selected NO_2 analysis window was 409 nm to 445 nm. The wavelength range was chosen because of lowest possible residual errors and DOAS fit result. For analysis, calibrated spectrum was used as reference spectrum. Different cross-sections: NO_2 at 298K (Vandaele et al., 1996), NO_2a at 220K (Vandaele et al., 1996), O_3 at 223K (Serdyuchenko, Gorshelev, Weber, Chehade, & Burrows, 2014), O_4 at 293K (Thalman & Volkamer, 2013), H_2O (Rothman & Transfer, 2010) and Ring were used. Polynomial of 4th degree was used for NO_2 analysis. Some fields/parameters in the "Output Tab" were selected which is required in the results i.e., Solar zenith Angle (SZA), RMS (root mean square/residue), Elevation viewing angle and integration time etc. Then finally, the output file path was given

where the files wanted to be stored. The analysis was performed on all measured spectra and NO_2 dSCDs and results were obtained in ASCII file.

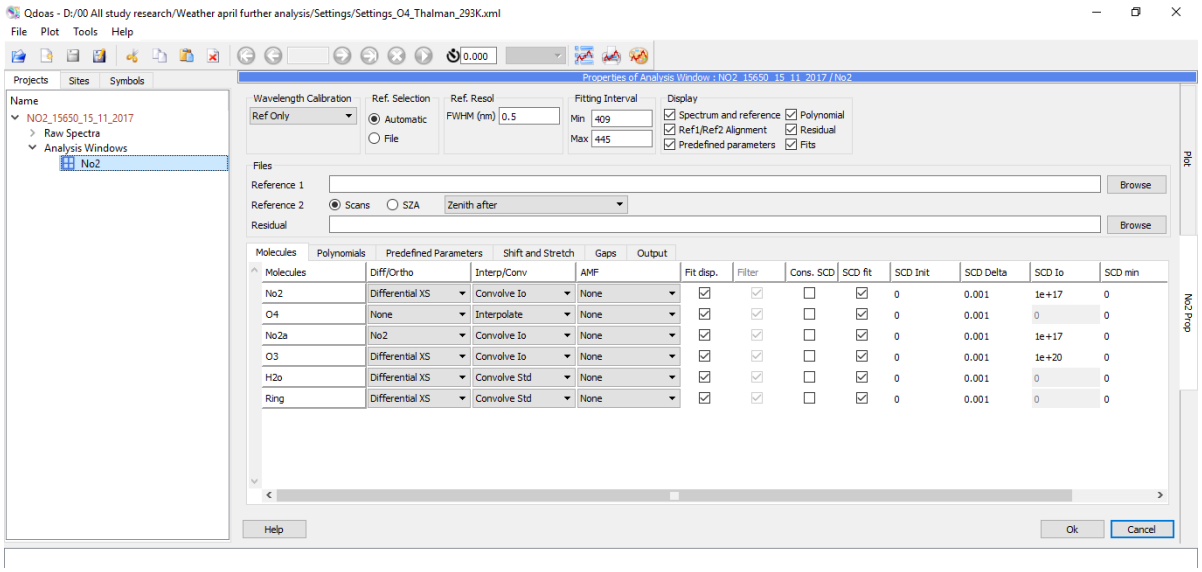

Figure 3.2 - NO2 Analysis window in QDOAS, showing fitting interval used for Nitrogen Dioxide

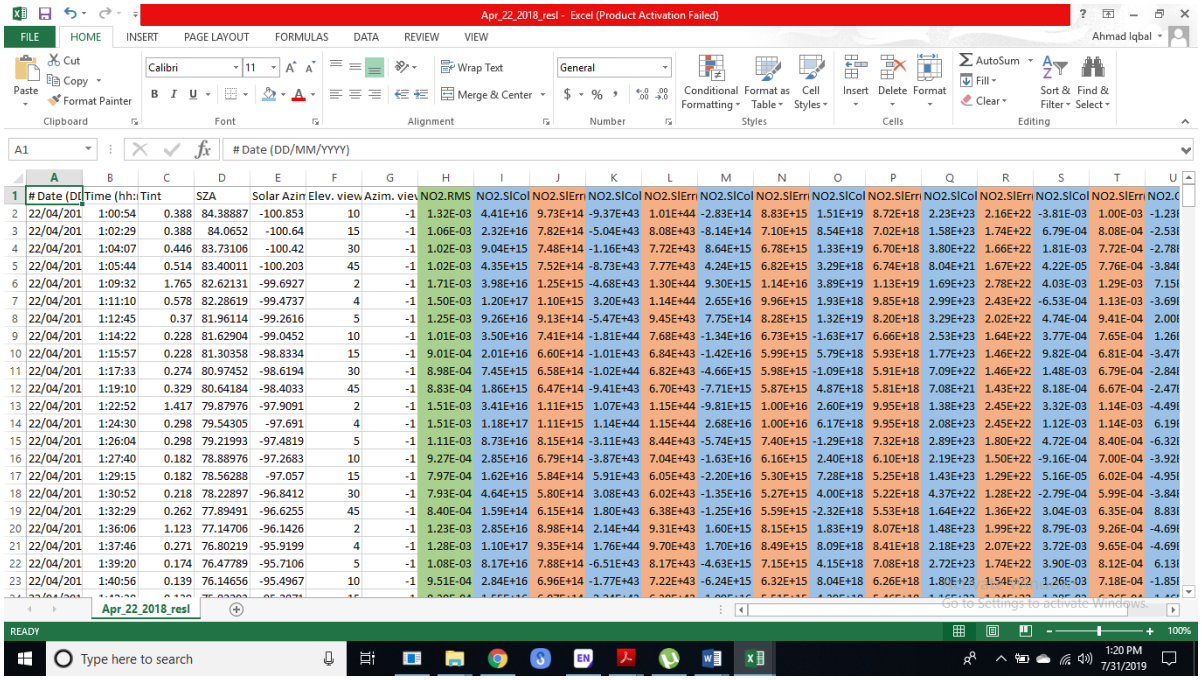

Figure 3.3 - ASCII files obtained by QDOAS; green column representing RMS, blue columns showing dSCDs, brown columns illustrate slant column errors

Figure 3.4 shows example of DOAS fit for NO_2. Red lines represents the reference spectrum and black line shows the measured spectrum after subtracting all other absorbers. It was

measured on 23 May 2018 at 12:36 UTC. SZA was 73° and elevation angle was 5°. Mean dSCD value for this fit was 3.55×10^{16} molecules cm^2.

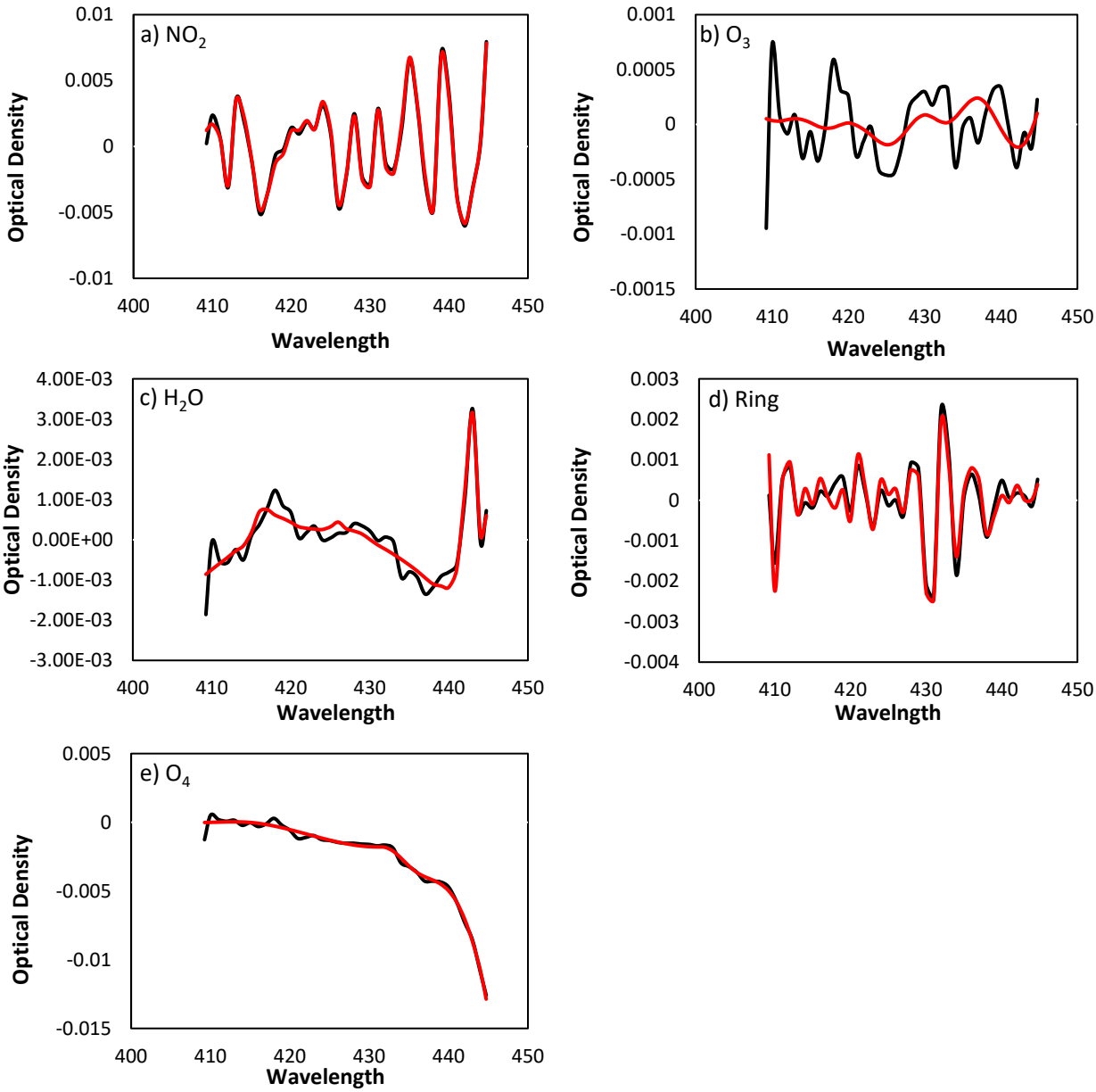

Figure 3.4- Nitrogen Dioxide DOAS fit measured on 23 May 2018 at 12:36 PST.

3.2.3. Air Mass Factor and NO_2 VCD Extraction Calculation using MS Excel

Microsoft Excel was used in this study to calculate NO_2 VCDs by using geometric air mass factor application. AMF is ratio of actual path distance of solar radiations and vertical path. AMF calculations are used to convert the SCDs (Slant column densities) into VCDs (Vertical

column densities). Air mass factor (AMF) is usually calculated using radiative transfer model but in this study, AMF was estimated using geometric approximation method (Hönninger et al., 2004; Wagner, Ibrahim, Shaiganfar, & Platt, 2010; Wittrock et al., 2004). This method allows the retrieval of column densities of trace gases even in cloudy conditions (Wagner et al., 2010).

$$VCD = SCD/AMF \quad \text{Eq. 9}$$

Here differential air mass factor (dAMF) is used because the slant column densities obtained were differential SCDs (Liu et al., 2016):

$$VCDtrop = dSCD\alpha / dAMF\alpha \quad \text{Eq. 10}$$

dAMF is difference in AMF obtained at a certain angle and AMF obtained at 90^o:

$$dAMF\alpha = AMF\alpha - AMF90° \quad \text{Eq. 11}$$

So, eq (10) will be:

$$VCD_{trop} = dSCD\alpha / AMF\alpha - AMF90° \quad \text{Eq. 12}$$

Using geometric approximation, AMF can be found as:

$$AMF = 1/\sin\alpha \quad \text{Eq. 13}$$

Then Eq. (12) will be:

$$VCD_{trop} = dSCD\alpha / 1/\sin(\alpha - 1) \quad \text{Eq. 14}$$

3.2.4. Validation of MAX-DOAS Observations by Satellite Data

For the validation and comparison of MAX-DOAS observations, Ozone Monitoring Instrument (OMI) observations were used for validation purpose. OMNO2d v003 product from TEMIS website was used (http://www.temis.nl/airpollution/no2.html). Data was downloaded in grid format (ESRI) and then Notepad++ was used to remove the values of -999 from the data. Then it was opened in ENVI software where it was converted into ERDAS Imagine Tagged image file format as shown in Figure 3.5. The tiffs were then opened and processed in

ArcGIS for value extraction at the specific location where the MAX-DOAS was mounted, furthermore both values of MAX-DOAS and Satellite were compared to validate the results of ground base monitoring of MAX-DOAS. For daily satellite data, OMNO2d v003 product from GIOVANNI website was downloaded in NetCDF format which was directly opened in ArcGIS by using "NetCDF to raster" tool.

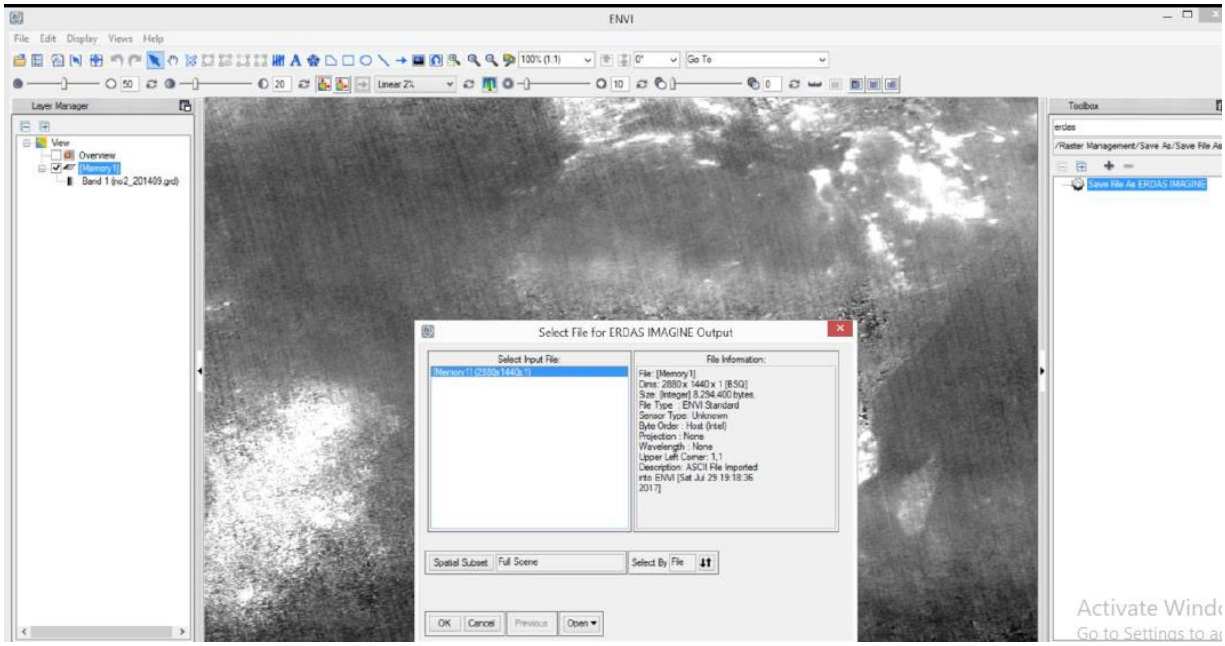

Figure 3.5 - Satellite data processing in ENVI

Chapter 4

4. RESULTS AND DISCUSSION:

4.1. Sensitive Study for optimum NO_2 settings:

NO_2 settings were implored in order to find the best settings with minimum root mean error of the residual. For this purpose, different polynomial orders and fitting interval were analyzed and results were compared with each other. In order to find optimum polynomial for best NO_2 retrieval settings, a range of polynomial orders from 3 to 7 were used on the same day whereas optimum polynomial degree is decided on the basis of root mean square of residual of NO_2 (RMS), slant column error and spectrum shift. Figure 4.1 shows RMS, shift (spectrum) and dSCD error (slant column error) plot against different polynomial order. It was found that RMS increased from 9.97e-04 to 1.02e-03, with decrease in polynomial order from 7 to one. However, Spectrum shift showed similar trend with lowest shift of 9.14e-04 and highest shift of 9.29e-04. Contrarily, NO_2 slant error showed inverse trend with RMS and spectrum shift. Lowest value was recorded at polynomial order 3 which is 6.94e+14. This value increased when higher polynomial orders were used in the settings showing directly proportional trend with polynomial order. Using high polynomial order can result in lower Shift in spectrum and lower RMS whereas higher slant column error.

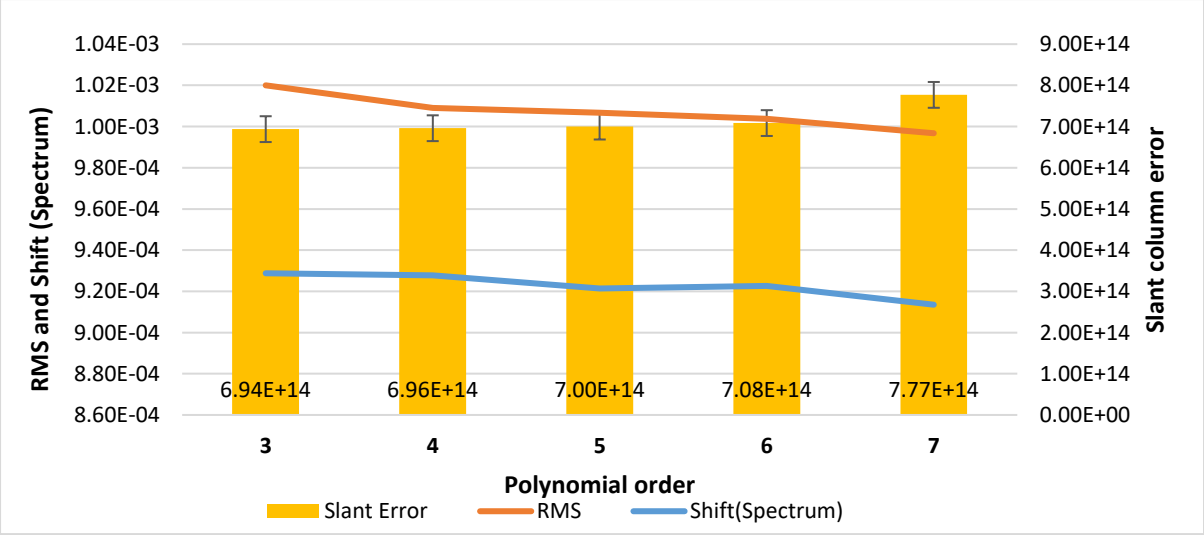

Figure 4.1 - Effect of Polynomial order on dSCD error, RMS and Shift Spectrum

Therefore, polynomial order 4 is optimum for NO_2 measurements as it shows minimum slant column error with least root mean square of residual and shift (spectrum). Then fourth degree polynomial was used in the settings of this study and comparison was carried out with other settings.

In order to find optimum fitting interval for NO_2, range of 330 to 445 was selected as it is range of spectrum measured by the instrument used in this study. At first, the upper boundary was kept constant at 445nm and lower boundary was increased from 330nm with the difference of 10nm up to 420nm. Then Lower boundary was kept constant at 330 nm and upper boundary was reduced with difference of 10nm up to 395 and results were recorded as shown in Table 4.1.

Table 4.1 - Results of NO_2 setting with different fitting intervals

Fitting Interval (nm)		Mean RMS	Mean dSCD	Mean dSCD error
Lower Boundary	Upper Boundary			
330	445	2.08E-03	6.32E+16	1.12E+15
340	445	1.93E-03	6.36E+16	1.04E+15
350	445	1.81E-03	6.40E+16	1.00E+15
360	445	1.72E-03	6.50E+16	9.79E+14
370	445	1.58E-03	6.48E+16	9.10E+14
380	445	1.39E-03	6.62E+16	8.27E+14
390	445	1.37E-03	6.58E+16	8.34E+14
400	445	1.03E-03	6.62E+16	6.95E+14
410	445	1.01E-03	6.55E+16	6.31E+14
420	445	1.01E-03	6.60E+16	8.20E+14
330	435	2.08E-03	6.10E+16	1.43E+15
330	425	2.03E-03	5.94E+16	1.67E+15
330	415	2.03E-03	5.90E+16	1.86E+15
330	405	2.03E-03	5.71E+16	2.35E+15
330	395	1.94E-03	5.39E+16	2.57E+15
330	385	1.66E-03	5.38E+16	2.35E+15
330	375	1.52E-03	5.81E+16	2.60E+15
330	365	1.48E-03	5.78E+16	2.94E+15
330	355	1.40E-03	5.75E+16	3.83E+15

It was observed that when upper boundary was kept constant at 445nm and lower boundary was increased. Values of Mean RMS decreased whereas mean dSCD were improved up to 410nm lower boundary. However, when lower boundary is kept constant, mean RMS

decreased with decrease in upper boundary but the values of mean dSCDs were also decreased, indicating that upper limit of 445nm is suitable for fitting interval. So, fitting interval from 410-445nnm was selected because of lowest mean RMS value and higher mean dSCD values as shown in Figure 4.2.

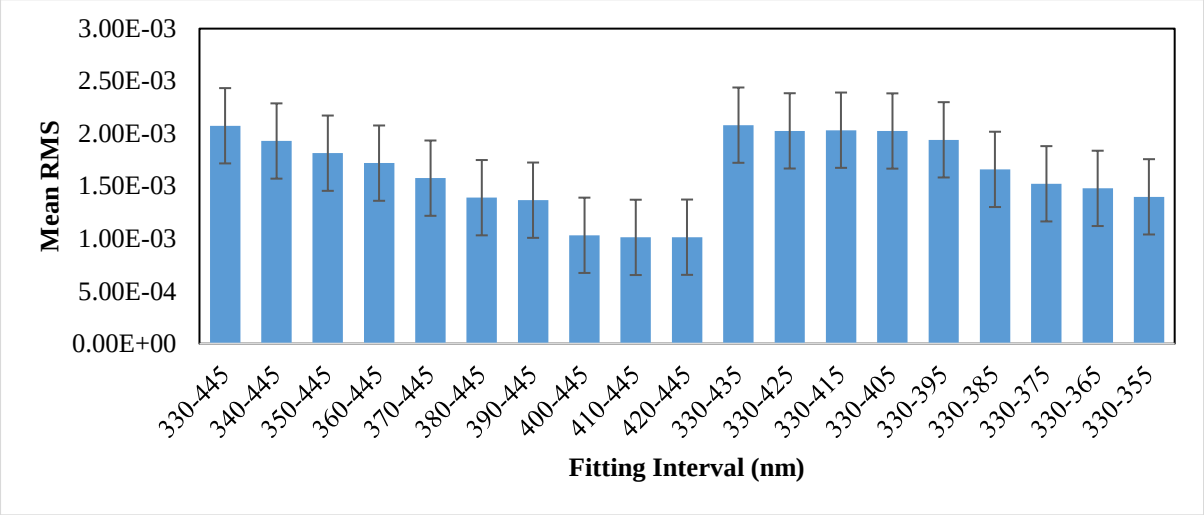

Figure 4.2 - Mean RMS values obtained at different fitting intervals

Further sensitive analysis was carried out, to further find the best fitting interval, by using lower boundary of fitting interval from 405nm to 415nm. It was observed that Figure 4.3 shows that 409-445nm fitting interval gives lowest RMS, so it was used in study to find NO_2 VCDs.

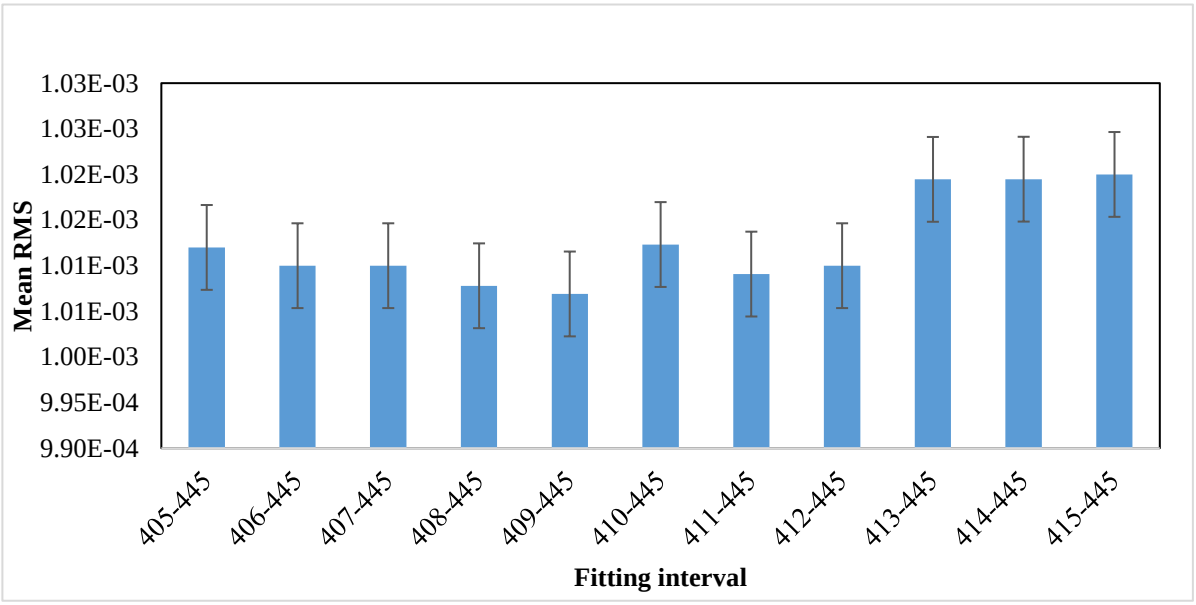

Figure 4.3 - Mean RMS values obtained from different lower boundary of fitting interval

4.2. Intercomparison of different settings

Nitrogen Dioxide (NO_2) has been in limelight of DOAS measurements due to its importance in atmospheric chemistry. The thing that makes this study unique is that it presents most of the settings that have been used in literature for NO_2 DOAS analysis along with their comparison to draw the best settings. Different of literature was consulted and settings reported in literature were recorded as shown in Table 4.2. Different settings were applied and spectral measurements of 1st November, 2017 were used in this comparative study.

Table 4.2 - List of the settings used for the retrieval of NO2 dSCDs on 01/11/2017.

Sr #	*Study*	*Wavelength (nm)*	*Absorber fitted*	*Maximum dSCD (Molecules/cm²)*	*Average dSCD (Molecules/cm²)*	*RMS*	*Spectrum shift*	*dSCD Error (Molecules/cm²)*
1	Tian et al. (2018)	338–360 nm	NO_2 (298 K) , NO_2 (220 K), O_3 (223 K), O_4 (293 K), BrO (223 k), SO_2 (294 K), HCHO (293 K), Ring	1.96E+17	6.42E+16	5.82E-04 - 6.13E-03	-5.26E-03 - 1.31E-03	4.14E+15
2	Jin et al. (2016)	405–430 nm	NO_2 (294 K), O_4 (296 K), Ring	2.09E+17	6.48E+16	4.30E-04 - 9.03E-03	-3.68E-04 - 8.91E-03	8.78E+14
3	Chong et al. (2016)	400–418 nm	NO_2 (294 K), O_3 (221 K), O_4 (298 K), Ring	2.09E+17	6.49E+16	3.73E-04 - 3.17E-03	-1.15E-03 - 5.19E-03	2.09E+15
4	Friedeburg et al. (2005)	420 and 450 nm	NO_2, Ring	2.14E+17	6.53E+16	4.53E-04 - 4.09E-03	-2.91E-04 - 3.62E-03	9.48E+14
5	Chan et al. (2015)	350.2 nm–386.6 nm	NO_2, O_4, O_3, HCHO, Ring	1.86E+17	5.31E+16	5.81E-04 - 5.42E-03	-2.10E-03 - 1.32E-03	2.49E+15
6	Lee et al. (2009)	364–383 nm	NO_2, O_4,O_3 (243 and 293 K), Ring	1.93E+17	5.27E+16	5.10E-04 - 5.25E-03	-2.05E-03 - 1.65E-03	2.68E+15
7	This Study	409–445nm	NO_2 (298 K), NO_2 (220 K), O_3 (223 K), O_4 (293 K), H_2O, Ring	2.17E+17	6.61E+16	4.53E-04 - 8.05E-03	-1.75E-04 - 5.79E-03	6.96E+14

This table indicates the results of settings use in this study along with settings found in this literature. Then dSCDs, RMS and slant column error obtained at 10^o was separated and plotted to observe the difference in results.

It was found that dSCDs of NO_2 obtained at elevation angle 10^o on 1 November, 2017 by using settings of this study were highest as compared to dSCDs obtained by using other settings

(Figure 4.4). Lowest values were recorded with settings of Lee et al however other values are slightly close to the values of settings of this study.

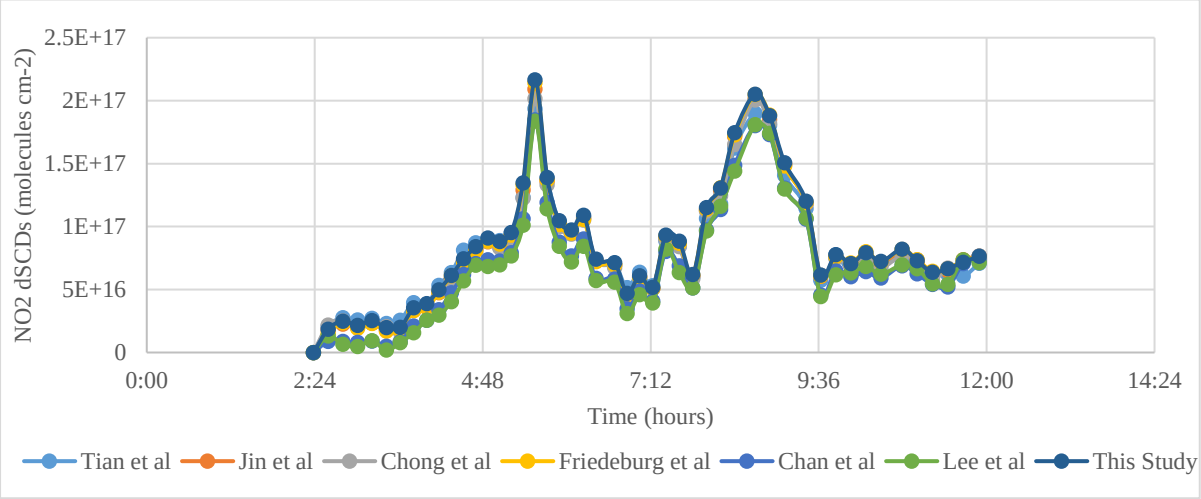

Figure 4.4 - Comparison of NO_2 dSCDs measured by using different settings reported in literature and this study.

RMS for dSCDs obtained by using the settings of this study was lower than that of Tian et al, Lee et al and Chan et al. While Friedelberg values were closer to the values obtained in this study and values of Jin et al. and Chong et al. were the lowest (Figure 4.5).

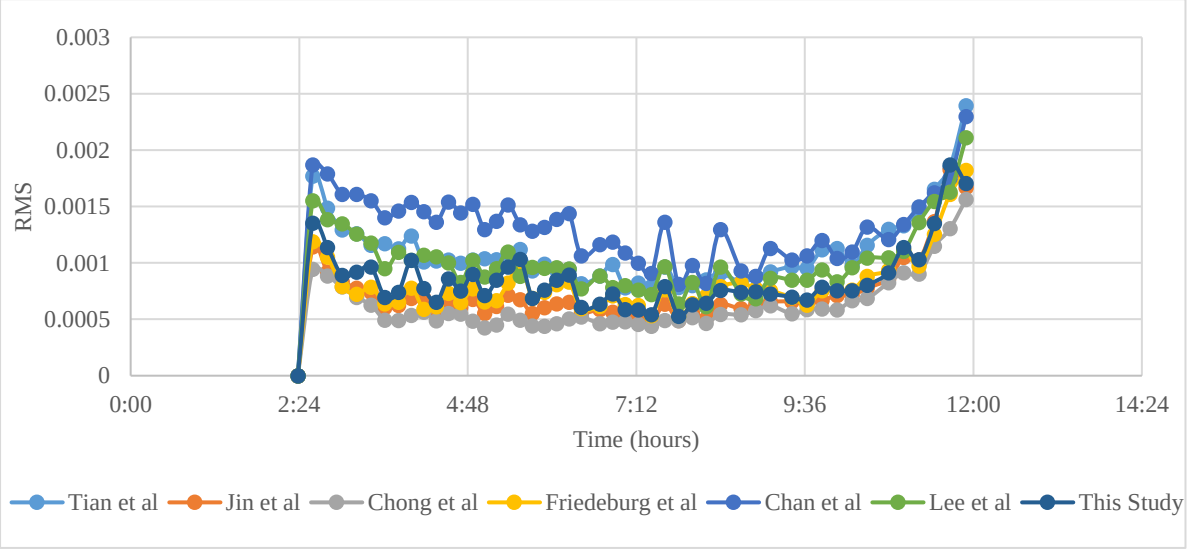

Figure 4.5 - Comparison of NO_2 RMS measured by using different settings reported in literature and this study

Slant column error obtained at 10^o from the results obtained from all settings were separated and then plotted to find the difference. It was found that slant column error obtained from the settings found through sensitive study was lowest. Whereas slant column error obtained by tian et al., settings was highest (Figure 4.6).

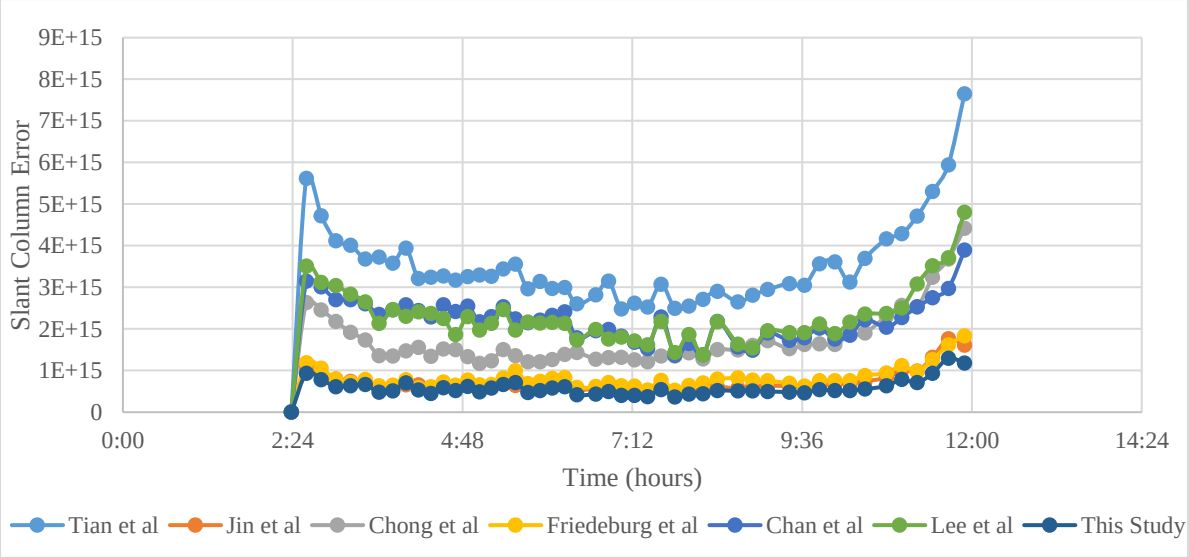

Figure 4.6 - Comparison of NO_2 slant column error measured by using different settings reported in literature and this study.

4.3. Correlation plots

For cross validation of settings used in this study, correlation was determined for this study's dSCDs against different settings mentioned in Table 1. DSCDs retrieved from different settings found in literature with settings used in this study were used to draw correlation plots which is shown in Figure 4.7. Highest correlation (Pearson value r = 0.999) is found with the settings of Jin et al. that includes strong NO_2 absorption band around 405–430 nm (see Table 1). However, other studies also show strong correlation with Pearson values (r) 0.987, 0.993, 0.998, 0.996, and 0.991 of Lee et al., Chan et al., Friedberg et al., Chong et al. and Tian et al. respectively. These results shows that the settings found through sensitive study for NO_2 are in line with the settings used in the literature.

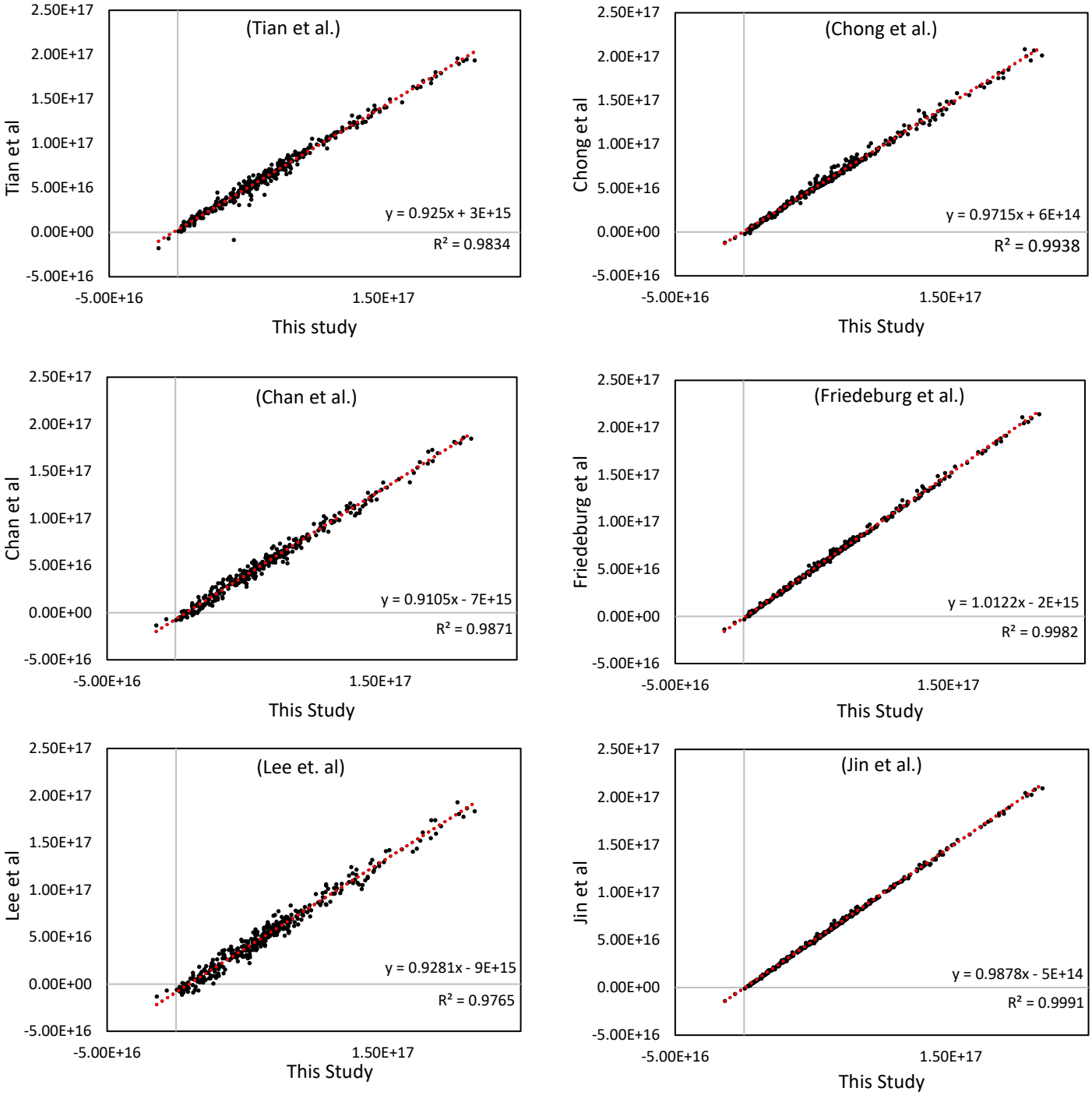

Figure 4.7 - Comparison of NO_2 slant column error measured by using different settings reported in literature and this study.

4.4. Intercomparison of different O_4 (Oxozone) cross-sections

Further analysis was carried out during cloudy conditions to find the impact of different Oxygen dimer (O_4) cross-sections on the retrieval of NO_2. For this purpose, four different O_4

cross-sections used were Burkholder et al., Hermans et al. 296K, Thalman 203K and Thalman 293K in settings of this study. DOAS fit of O_3 and O_4 were chosen as a criteria for finding the impact. Figure 4.8 shows the comparison of O_3 spectrum obtained by different O_4 and it can be seen that Brukholder O_4 Cross-section improved the fitting of measured spectrum. However, Figure 4.9 also depicts the improvement in fitting of measured and reference spectrum for O_4. Mean RMS values obtained with different cross-sections were 2.2042×10^{-3}, 2.2045×10^{-3}, 2.2093×10^{-3} and 2.2092×10^{-3} for Brukholder, Hermans, Thalman 203K and Thalman 293K, respectively. It also shows slight decrease in root mean square error which is also one of the indicators of the quality of DOAS fit settings. Therefore, it can be observed that of these cross-sections, using Brukholder et al. O_4 cross-section improves the DOAS fit results when used for the retrieval of NO_2 dSCDs.

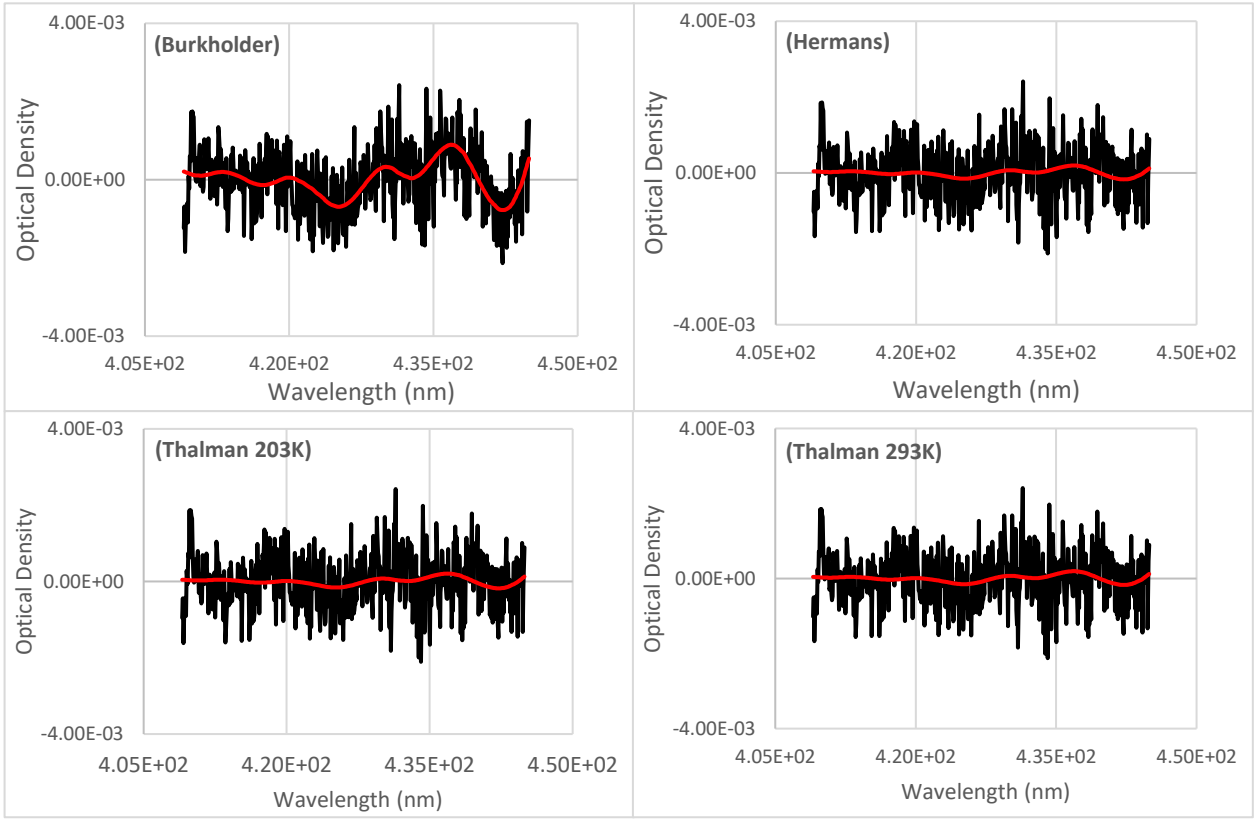

Figure 4.8 - A comparison of O_3 DOAS fit spectrum for different O_4 cross-sections where black lines depicts measured spectrum and red line shows reference spectrum.

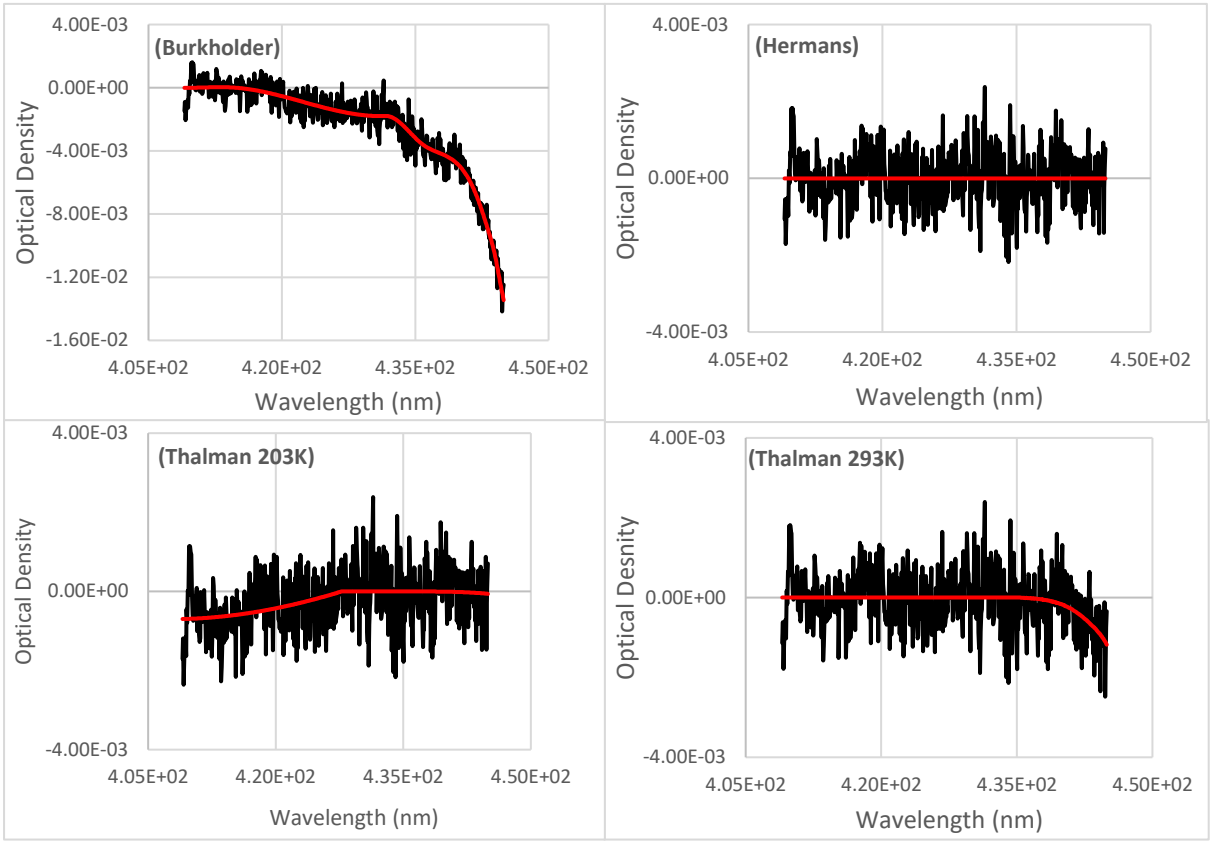

Figure 4.9 - A comparison of O_4 DOAS fit spectrum for different O_4 cross-sections where black lines depicts measured spectrum and red line shows reference spectrum

4.5. Effect of different meteorological conditions on RMS, dSCD Error and spectrum shift.

The settings for analysis of this study are used to explore the behavior of DOAS NO_2 fit during the effect of haze, clear and cloudy conditions. According to Surface Meteorological Observation Specification (CMA, 2003), Haze occurs when relative humidity is >80% and visibility is <10 km. Based on meteorological conditions, 22 April, 26 April and 23 May 2018 were chosen for this analysis as hazy, cloudy and clear days, respectively (Hong et al., 2016; Liu et al., 2016). Table 4.3 Displays average values of DOAS fit parameters during these days. It shows that dSCD of NO_2 obtained during cloudy day is higher as compared to clear and hazy day. Meanwhile, clear day dSCD is lowest among the three.

Table 4.3 - Effect of haze, clear and cloudy days on different parameters

Date	Condition	Humidity (%)	Mean Air Temperature (F°)	Mean visibility (miles)	Mean RMS ($x10^{-3}$)	Mean dSCD (molecule/cm^2)	Mean DSCD error	Mean Spectrum Shift
22-04-18	Hazy	46%	74°F	3	1.09	4.01E+16	7.40E+14	1.18E-03
26-04-18	Cloudy	33%	84°F	10	1.23	4.15E+16	8.33E+14	1.35E-03
23-05-18	Clear	31%	88°F	23	2.21	3.56E+16	1.47E+15	-1.98E-03

Figure 4.10 shows that there is no significant change in RMS and Shift of Hazy and Cloudy day. However, RMS and shift spectrum values obtained were lower in clear day than that of hazy and cloudy day.

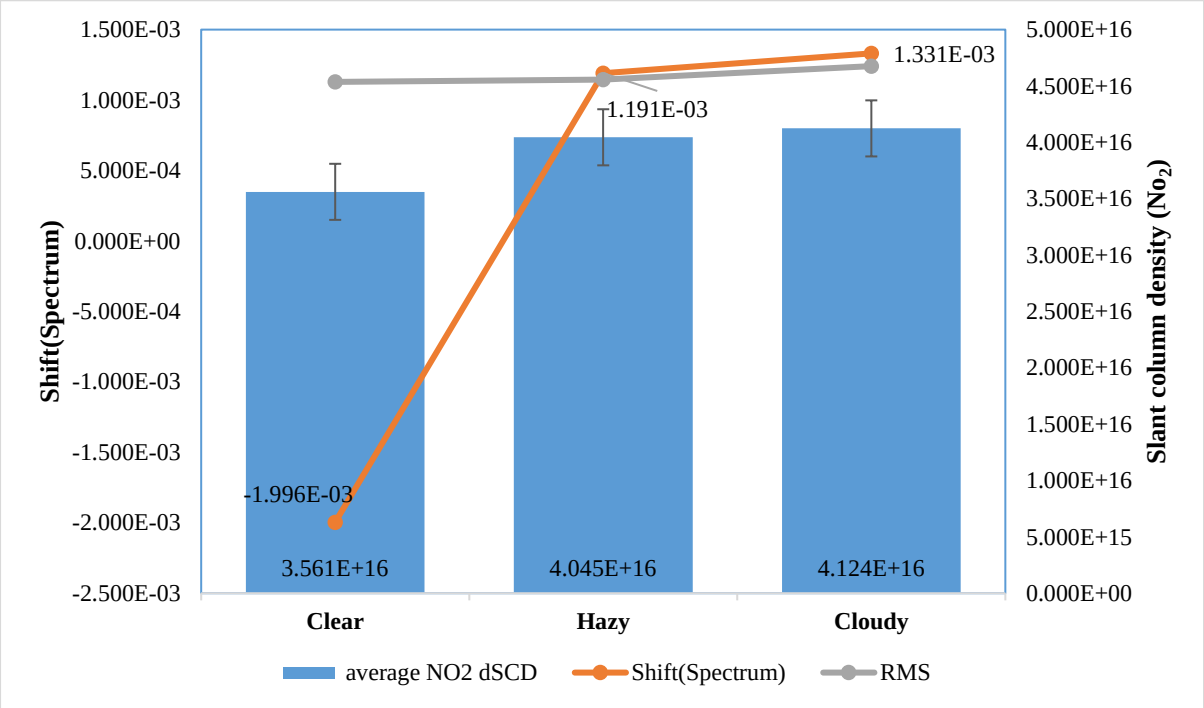

Figure 4.10 - Effect of Hazy, Cloudy and Clear days on RMS, Shift and dSCDs

In the presence of radiation, NO_2 readily breaks down into NO in atmosphere. Results of NO2 slant column densities obtained on clear condition showed the same. It can be explained as during clear day, photo-dissociation of NO_2 takes place in the presence of light where as in cloudy days less radiation is available that results in accumulation of NO_2 in atmosphere. In hazy scenario, solar light is available but it is in diffused form due to fine particle that makes condition hazy (Zhang et al., 2015). Spectrum shift and RMS followed the same trend as that of the dSCDs trend during different meteorological conditions.

4.6. Comparison of observations with OMI data:

Data from Ozone Monitoring Instrument (OMI) was taken for 22 April, 26 April and 23 May, 2018 in order to validate the MAX-DOAS measurements. OMI is aboard AURA satellite and its daily overpass time is 13:40 local time. Resolution of OMI data is 13x24km^2 and its

observations are always average value. OMI measurements for 22 April, 26 April and 23 May were compared with the VCDs of respective days as shown in Figure 4.11. It can be observed that OMI observations are low as compared to the measurements obtained by ground based MAX-DOAS. This underestimation is mainly attributed to the shielding effect of aerosols, clouds and coarse resolution of the OMI ground-pixel(Ma et al., 2013). Comparison of Monthly variation was also showed the underestimation as shown in Figure 4.12.

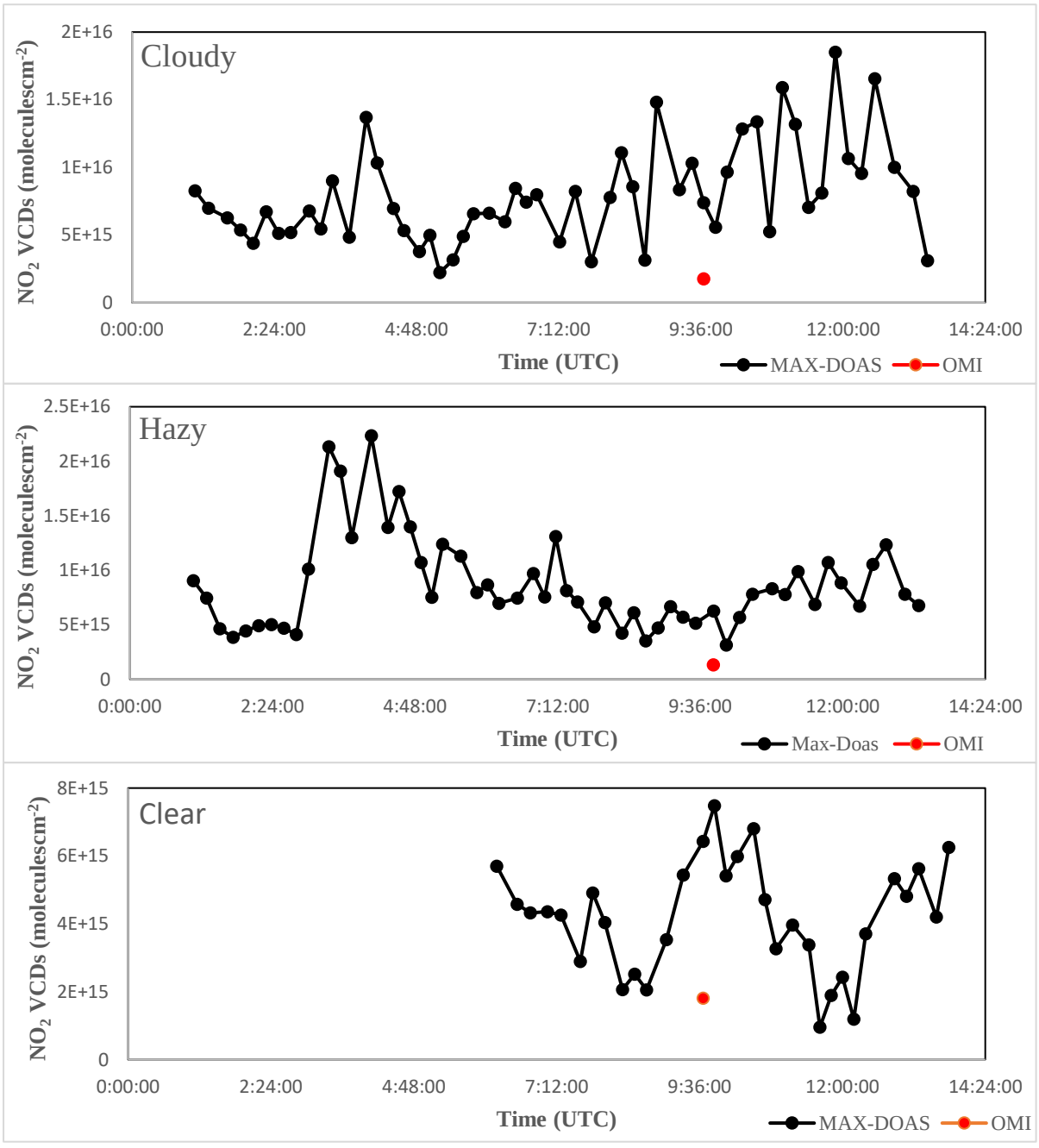

Figure 4.11 - Comparison of MAX-DOAS measurements with OMI data.

Through Figure 4.12, the annual trend of NO_2 is apparent as low concentration in summer (May-August) whereas high concentration during winter season (December-March). Moreover, satellite observations shows the same trend as that of ground observations. Correlation of ground based and Satellite data shows low Pearson value i.e. 0.733 Figure 4.13 - a. It can be attributed to the difference in observation timings of both. In order to improve the Pearson value (r), average of ground based data from 12pm to 2pm was used to carry out the correlation and results improved the Pearson value as shown in Figure 4.13 - b. Result were made significant, with r = 0.843 (Figure 4.13 - c), by taking the average of 1pm to 2pm of ground based data as satellite passing time site of the study is around 1:40pm. However, spatial resolution of satellite observation can also be a contributing factor for underestimation as OMI satellite's spatial resolution is 13x24 km^2 which shows the concentration over a larger area as compared to the ground based point observations.

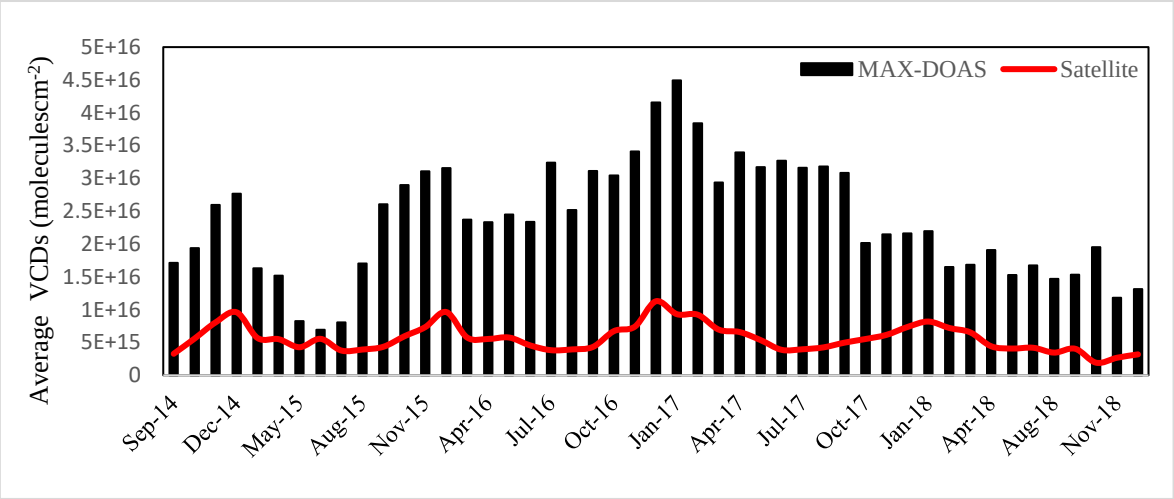

Figure 4.12 - Comparison of MAX-DOAS and Satellite monthly observations.

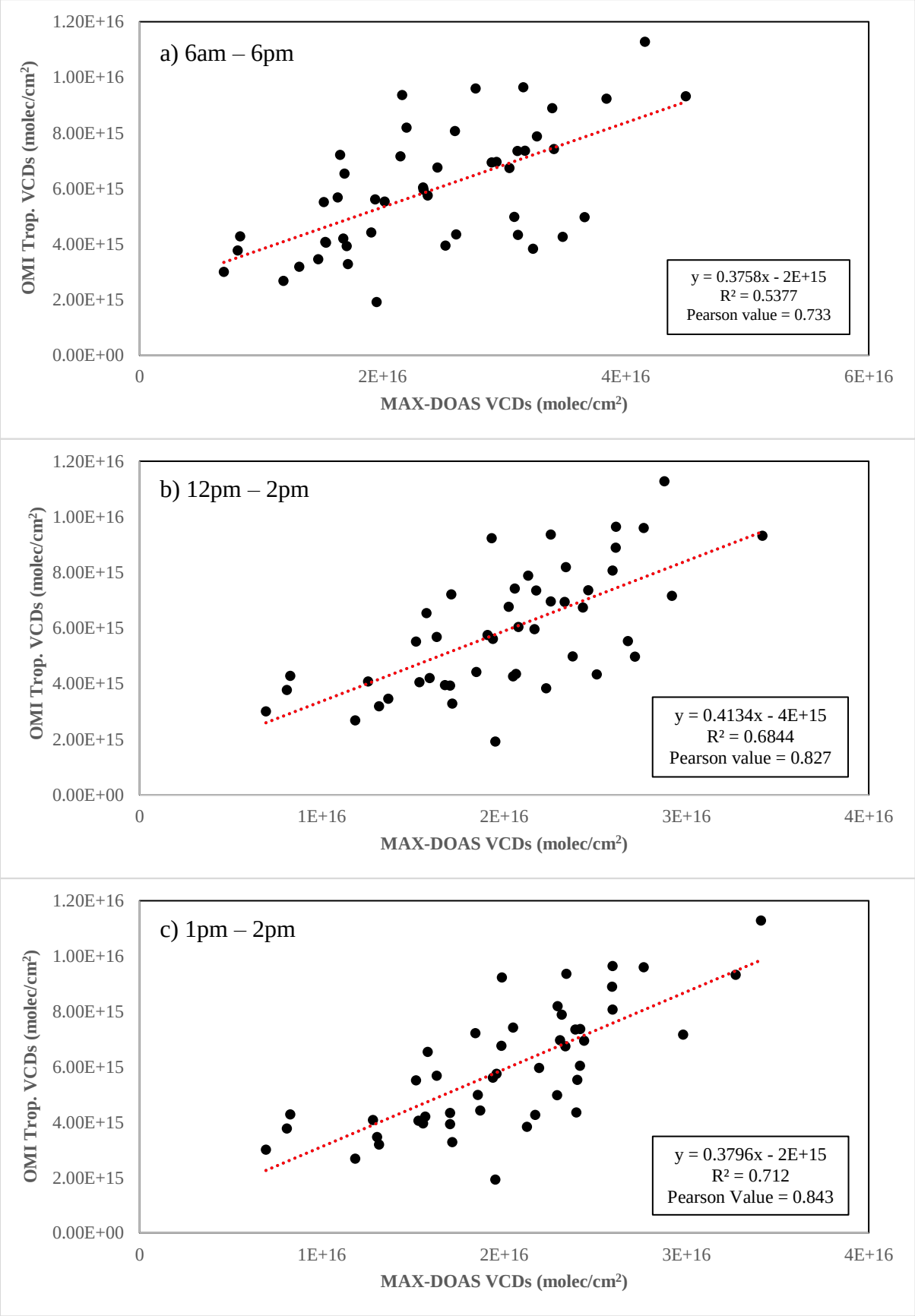

Figure 4.13 - Correlation plots between Satellite data and ground based observations.

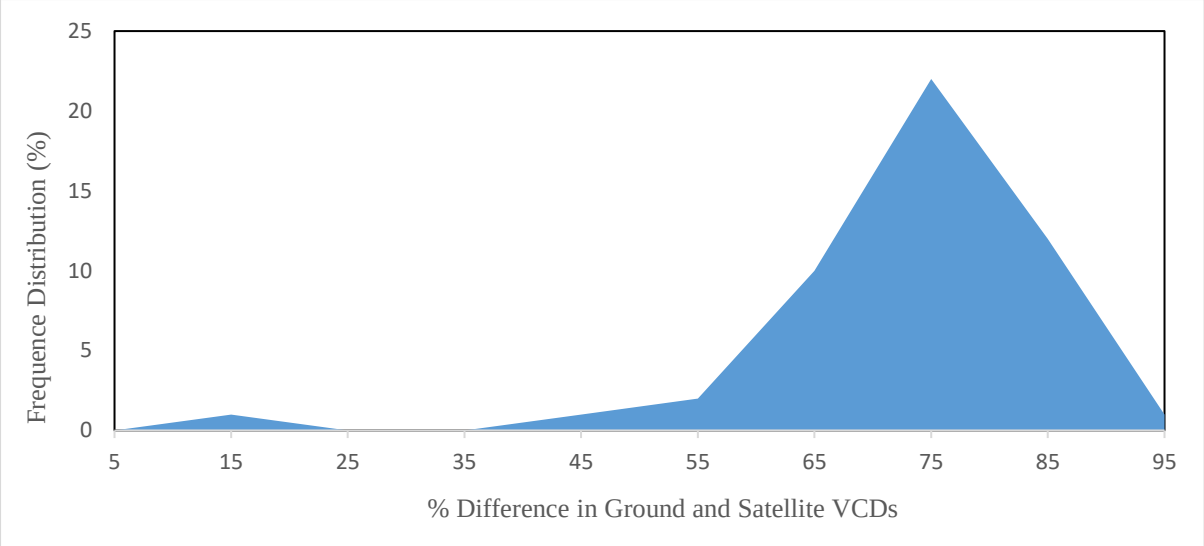

Figure 4.14 - Frequency Histogram of percentage difference between MAX-DOAS and Satellite observations.

A frequency histogram was also produced between MAX-DOAS and Satellite data to find the frequency of percentage difference between both observations. The histogram exhibits a percentage difference distribution peaking at around 75% with almost 90% of the data lying between 45% and 95% of the difference (Figure 4.14)

Chapter 5

5. CONCLUSION AND RECOMMENDATIONS:

5.1. Conclusion

Very few studies have been conducted on hazy, clear and cloudy days. NO_2 is important trace gas due to its active role in atmospheric chemistry. It plays important role in catalytic formation of ozone in troposphere as well as it is one of the precursors of photochemical smog. In this study comparison of different polynomial degree was carried out and order 4 was chosen for this study on the basis of least RMS and dSCD error. Different NO_2 retrieval settings found in literature were then compared with settings used in this study for 01 November 2017. Correlation plots showed good agreement among the measurements with least R^2 =0.97 (0.98). Another analysis was carried out during different meteorological conditions i.e. hazy, cloudy and clear days to explore the behavior of NO_2 DOAS fit during. NO_2 in atmosphere dissociates in the presence of sunlight which is major reason for its shorter lifetime in atmosphere. Results from this showed lower concentration of NO_2 during clear day. Whereas during cloudy and hazy conditions concentrations are slightly higher as lesser and diffused light is available in such conditions. Furthermore, different O_4 cross-sections were used to investigate the impact on DOAS fit. Cross section of Burkholder et al., (1994) showed lowest RMS in measurements and improved the DOAS fits of O_3 and O_4. For validation of the observations, ground based observations were compared with OMI satellite data which showed satellite observations underestimate NO_2 columns largely. Further comparison from 2014 to 2018 data also showed the same trend with 22% of the observations having difference of 75%.

5.2. Recommendations

Some recommendations based on the outcome from this study are made includes as following:

1. The outcomes of this study helped to identify the behavior of nitrogen dioxide during special weather conditions, therefore, such studies can be carried out to find the behavior of other air pollutants in such conditions. It will contribute in better understanding of the problem.

2. Study can be replicated to find optimum settings of different trace gases such as SO_2, O_3.

3. This study's outcome shows the increased NO_2 concentration during hazy and cloudy condition as compared to that of clear days. It is due to aggregation of NO_2 in atmosphere when light is absent or in other words, photo dissociation of NO_2 stops. It is also attributed to increased fossil fuel consumption in transportation as it is major source of NO_2 in Pakistan. NO_2 can be checked and kept low by reducing our dependency on fossil fuels. It can be done by focusing on green technology, like installation of catalytic converters in vehicles, and relying on renewable energy resources.

4. Public transport system should be developed in rural and urban areas to reduce traffic congestion and load. Vehicular emission can also be improved by proper maintenance of vehicles. Proper vehicular maintenance check should be carried out on regular basis.

5. Ambient air quality should be monitored on continuous basis through a proper management plan and baseline data should be developed of at least major cities. It should be shared publically which will help in educating the locals about emission levels and pollution sources.

6. Effective media/awareness campaigns should be carried out to teach public and other stakeholders for better understanding of ambient air pollution issues. Different groups and school children can be targeted during these campaigns and causes, impacts and remedies should be discussed to impart sense of responsibility among them.

References

Akimoto, H. J. S. (2003). Global air quality and pollution. *302*(5651), 1716-1719.

Ali, M., Athar, M. J. E. m., & Assessment. (2008). Air pollution due to traffic, air quality monitoring along three sections of National Highway N-5, Pakistan. *136*(1-3), 219-226.

Badr, O., & Probert, S. J. A. e. (1993). Oxides of nitrogen in the earth's atmosphere: trends, sources, sinks and environmental impacts. *46*(1), 1-67.

Bang, H. Q., Nguyen, H. D., Vu, K., Hien, T. T. J. E. M., & Assessment. (2018). Photochemical Smog Modelling Using the Air Pollution Chemical Transport Model (TAPM-CTM) in Ho Chi Minh City, Vietnam. 1-16.

Beard, B. A., & Freas, W. P. J. E. S. A. F. (1994). National Air Quality and Emissions Trends Report. *163*.

Beelen, R., Hoek, G., Vienneau, D., Eeftens, M., Dimakopoulou, K., Pedeli, X., . . . Marcon, A. J. A. E. (2013). Development of NO2 and NOx land use regression models for estimating air pollution exposure in 36 study areas in Europe–The ESCAPE project. *72*, 10-23.

Beirle, S., Platt, U., Wenig, M., Wagner, T. J. A. C., & Physics. (2003). Weekly cycle of NO 2 by GOME measurements: A signature of anthropogenic sources. *3*(6), 2225-2232.

Bobrowski, N., Hönninger, G., Galle, B., & Platt, U. J. N. (2003). Detection of bromine monoxide in a volcanic plume. *423*(6937), 273.

Boynard, A., Clerbaux, C., Clarisse, L., Safieddine, S., Pommier, M., Van Damme, M., . . . Hurtmans, D. J. G. R. L. (2014). First simultaneous space measurements of atmospheric pollutants in the boundary layer from IASI: A case study in the North China Plain. *41*(2), 645-651.

Brasseur, G. P., & Solomon, S. (2006). *Aeronomy of the middle atmosphere: chemistry and physics of the stratosphere and mesosphere* (Vol. 32): Springer Science & Business Media.

Brook, R. D., Brook, J. R., Urch, B., Vincent, R., Rajagopalan, S., & Silverman, F. J. C. (2002). Inhalation of fine particulate air pollution and ozone causes acute arterial vasoconstriction in healthy adults. *105*(13), 1534-1536.

Burrows, J. P., Platt, U., & Borrell, P. (2011). *The remote sensing of tropospheric composition from space*: Springer Science & Business Media.

Chan, K., Hartl, A., Lam, Y., Xie, P., Liu, W., Cheung, H., . . . Xu, J. J. A. E. (2015). Observations of tropospheric NO2 using ground based MAX-DOAS and OMI measurements during the Shanghai World Expo 2010. *119*, 45-58.

Chan, K., Wiegner, M., Wenig, M., & Pöhler, D. J. S. o. t. t. e. (2018). Observations of tropospheric aerosols and NO2 in Hong Kong over 5 years using ground based MAX-DOAS. *619*, 1545-1556.

Chan, K. L., Wang, Z., Ding, A., Heue, K.-P., Shen, Y., Wang, J., . . . Wenig, M. J. A. C. P. D. (2019). MAX-DOAS measurements of tropospheric NO 2 and HCHO in Nanjing and the comparison to OMI observations.

Chen, X., Wang, F., Hyun, J. Y., Wei, T., Qiang, J., Ren, X., . . . Yoon, J. J. C. S. R. (2016). Recent progress in the development of fluorescent, luminescent and colorimetric probes for detection of reactive oxygen and nitrogen species. *45*(10), 2976-3016.

Cheng, S., Ma, J., Cheng, W., Yan, P., Zhou, H., Zhou, L., & Yang, P. J. J. o. E. S. (2019). Tropospheric NO2 vertical column densities retrieved from ground-based MAX-DOAS measurements at Shangdianzi regional atmospheric background station in China. *80*, 186-196.

Clémer, K., Van Roozendael, M., Fayt, C., Hendrick, F., Hermans, C., Pinardi, G., . . . De Mazière, M. J. A. M. T. (2010). Multiple wavelength retrieval of tropospheric aerosol optical properties from MAXDOAS measurements in Beijing. *3*(4), 863.

Coburn, S., Dix, B., Sinreich, R., & Volkamer, R. J. A. M. T. (2011). The CU ground MAX-DOAS instrument: characterization of RMS noise limitations and first measurements near Pensacola, FL of BrO, IO, and CHOCHO. *4*(11), 2421-2439.

Demirel, G., Özden, Ö., Döğeroğlu, T., & Gaga, E. O. J. S. o. t. t. e. (2014). Personal exposure of primary school children to BTEX, NO2 and ozone in Eskişehir, Turkey: Relationship with indoor/outdoor concentrations and risk assessment. *473*, 537-548.

Dix, B., Koenig, T., & Volkamer, R. J. A. M. T. (2016). Parameterization retrieval of trace gas volume mixing ratios from Airborne MAX-DOAS. *9*(11).

Dockery, D. W., Pope, C. A., Xu, X., Spengler, J. D., Ware, J. H., Fay, M. E., . . . Speizer, F. E. J. N. E. j. o. m. (1993). An association between air pollution and mortality in six US cities. *329*(24), 1753-1759.

Dockery, D. W., & Pope, C. A. J. A. r. o. p. h. (1994). Acute respiratory effects of particulate air pollution. *15*(1), 107-132.

Drummond, J. W., Volz, A., & Ehhalt, D. H. J. J. o. a. c. (1985). An optimized chemiluminescence detector for tropospheric NO measurements. *2*(3), 287-306.

Finlayson-Pitts, B. J., & Pitts, J. N. J. S. (1997). Tropospheric air pollution: ozone, airborne toxics, polycyclic aromatic hydrocarbons, and particles. *276*(5315), 1045-1051.

Fioletov, V., McLinden, C., Krotkov, N., Yang, K., Loyola, D., Valks, P., . . . Chance, K. J. J. o. G. R. A. (2013). Application of OMI, SCIAMACHY, and GOME-2 satellite SO2 retrievals for detection of large emission sources. *118*(19), 11,399-311,418.

Fontijn, A., Sabadell, A. J., & Ronco, R. J. J. A. c. (1970). Homogeneous chemiluminescent measurement of nitric oxide with ozone. Implications for continuous selective monitoring of gaseous air pollutants. *42*(6), 575-579.

Frins, E., Bobrowski, N., Osorio, M., Casaballe, N., Belsterli, G., Wagner, T., & Platt, U. J. A. e. (2014). Scanning and mobile multi-axis DOAS measurements of SO2 and NO2 emissions from an electric power plant in Montevideo, Uruguay. *98*, 347-356.

Grosjean, D., Harrison, J. J. E. s., & technology. (1985). Response of chemiluminescence NOx analyzers and ultraviolet ozone analyzers to organic air pollutants. *19*(9), 862-865.

Guenther, A., Geron, C., Pierce, T., Lamb, B., Harley, P., & Fall, R. J. A. E. (2000). Natural emissions of non-methane volatile organic compounds, carbon monoxide, and oxides of nitrogen from North America. *34*(12-14), 2205-2230.

Habeebullah, T. M., Munir, S., Morsy, E. A., & Mohammed, A. M. (2010). *Spatial and temporal analysis of air pollution in Makkah, the Kingdom of Saudi Arabia.* Paper presented at the 5th International Conference on Environmental Science and Technology, IPCBEE, ISSN.

Halla, J., Wagner, T., Beirle, S., Brook, J., Hayden, K., O'brien, J., . . . Physics. (2011). Determination of tropospheric vertical columns of NO 2 and aerosol optical properties in a rural setting using MAX-DOAS. *11*(23), 12475-12498.

Han, X., & Naeher, L. P. J. E. i. (2006). A review of traffic-related air pollution exposure assessment studies in the developing world. *32*(1), 106-120.

Hendrick, F., Müller, J.-F., Clémer, K., Wang, P., Mazière, M. D., Fayt, C., . . . Physics. (2014). Four years of ground-based MAX-DOAS observations of HONO and NO 2 in the Beijing area. *14*(2), 765-781.

Hilboll, A., Richter, A., Burrows, J. J. A. C., & Physics. (2013). Long-term changes of tropospheric NO2 over megacities derived from multiple satellite instruments. *13*(8), 4145.

Holton, J. R., Haynes, P. H., McIntyre, M. E., Douglass, A. R., Rood, R. B., & Pfister, L. J. R. o. g. (1995). Stratosphere-troposphere exchange. *33*(4), 403-439.

Hong, Q., Xie, Z., Liu, C., Wang, F., Xie, P., Kang, H., . . . Physics. (2016). Speciated atmospheric mercury on haze and non-haze days in an inland city in China. *16*(21), 13807-13821.

Hönninger, G., Friedeburg, C. v., Platt, U. J. A. C., & Physics. (2004). Multi axis differential optical absorption spectroscopy (MAX-DOAS). *4*(1), 231-254.

Ibrahim, O. (2009). *Applications on Ground-based Tropospheric Measurements using Multi-Axis Differential Optical Absorption Spectrosopy.*

Irie, H., Kanaya, Y., Akimoto, H., Tanimoto, H., Wang, Z., Gleason, J., . . . Physics. (2008). Validation of OMI tropospheric NO 2 column data using MAX-DOAS measurements deep inside the North China Plain in June 2006: Mount Tai Experiment 2006. *8*(22), 6577-6586.

Jahangir, S., Ahmad, S. S., Aziz, N., Shah, M. T. A. J. J. o. I. E. A., & Science. (2013). Spatial variation of nitrogen dioxide concentration in private and public hospitals of Rawalpindi and Islamabad, Pakistan. *8*, 16-24.

Khan, W. A., Khokhar, M. F., Shoaib, A., & Nawaz, R. J. A. P. R. (2018). Monitoring and analysis of formaldehyde columns over Rawalpindi-Islamabad, Pakistan using MAX-DOAS and satellite observation. *9*(5), 840-848.

Khokhar, M., Naveed, S., Butt, J., & Abbas, Z. J. A. (2016). Comparative analysis of atmospheric glyoxal column densities retrieved from MAX-DOAS observations in Pakistan and during MAD-CAT field campaign in Mainz, Germany. *7*(5), 68.

Kreher, K., Van Roozendael, M., Hendrick, F., Apituley, A., Dimitropoulou, E., Frieß, U., . . . Ang, L. (2019). Intercomparison of NO2, O4, O3 and HCHO slant column measurements by MAX-DOAS and zenith-sky UV-Visible spectrometers during the CINDI-2 campaign.

Lee, C., Martin, R. V., van Donkelaar, A., Lee, H., Dickerson, R. R., Hains, J. C., . . . Schwab, J. J. J. J. o. G. R. A. (2011). SO2 emissions and lifetimes: Estimates from inverse modeling using in situ and global, space-based (SCIAMACHY and OMI) observations. *116*(D6).

Leser, H., Hönninger, G., & Platt, U. J. G. R. L. (2003). MAX-DOAS measurements of BrO and NO2 in the marine boundary layer. *30*(10).

Li, C., Zhang, Q., Krotkov, N. A., Streets, D. G., He, K., Tsay, S. C., & Gleason, J. F. J. G. R. L. (2010). Recent large reduction in sulfur dioxide emissions from Chinese power plants observed by the Ozone Monitoring Instrument. *37*(8).

Li, X., Brauers, T., Hofzumahaus, A., Lu, K., Li, Y., Shao, M., . . . Physics. (2013). MAX-DOAS measurements of NO 2, HCHO and CHOCHO at a rural site in Southern China. *13*(4), 2133-2151.

Lin, J.-T., Martin, R., Boersma, K., Sneep, M., Stammes, P., Spurr, R., . . . Physics. (2014). Retrieving tropospheric nitrogen dioxide from the Ozone Monitoring Instrument: effects of aerosols, surface reflectance anisotropy, and vertical profile of nitrogen dioxide. *14*(3), 1441-1461.

Lin, J.-T., McElroy, M. B. J. A. C., & Physics. (2011). Detection from space of a reduction in anthropogenic emissions of nitrogen oxides during the Chinese economic downturn. *11*(15), 8171-8188.

Liu, Q., Ma, T., Olson, M. R., Liu, Y., Zhang, T., Wu, Y., & Schauer, J. J. J. S. r. (2016). Temporal variations of black carbon during haze and non-haze days in Beijing. *6*, 33331.

Lohberger, F., Hönninger, G., & Platt, U. J. A. o. (2004). Ground-based imaging differential optical absorption spectroscopy of atmospheric gases. *43*(24), 4711-4717.

Lübken, F. J. J. J. o. G. R. A. (1999). Thermal structure of the Arctic summer mesosphere. *104*(D8), 9135-9149.

Ma, J., Beirle, S., Jin, J., Shaiganfar, R., Yan, P., Wagner, T. J. A. C., & Physics. (2013). Tropospheric NO 2 vertical column densities over Beijing: results of the first three years of ground-based MAX-DOAS measurements (2008–2011) and satellite validation. *13*(3), 1547-1567.

Martin, R. V. J. A. e. (2008). Satellite remote sensing of surface air quality. *42*(34), 7823-7843.

Pandey, J. S., Kumar, R., & Devotta, S. J. A. E. (2005). Health risks of NO2, SPM and SO2 in Delhi (India). *39*(36), 6868-6874.

Parekh, P. P., Khwaja, H. A., Khan, A. R., Naqvi, R. R., Malik, A., Shah, S. A., . . . Hussain, G. J. A. E. (2001). Ambient air quality of two metropolitan cities of Pakistan and its health implications. *35*(34), 5971-5978.

Peters, E., Wittrock, F., Großmann, K., Frieß, U., Richter, A., Burrows, J. J. A. C., & Physics. (2012). Formaldehyde and nitrogen dioxide over the remote western Pacific Ocean: SCIAMACHY and GOME-2 validation using ship-based MAX-DOAS observations. *12*(22), 11179-11197.

Pikelnaya, O., Hurlock, S. C., Trick, S., & Stutz, J. J. J. o. G. R. A. (2007). Intercomparison of multiaxis and long-path differential optical absorption spectroscopy measurements in the marine boundary layer. *112*(D10).

Platt, U., & Stutz, J. (2008). Differential Optical Absorption Spectroscopy Principles and Applications. In *Differential Optical Absorption Spectroscopy* (pp. 135-174): Springer.

Pollack, I. B., Lerner, B. M., & Ryerson, T. B. J. J. o. a. c. (2010). Evaluation of ultraviolet light-emitting diodes for detection of atmospheric NO 2 by photolysis-chemiluminescence. *65*(2-3), 111-125.

Pope III, C. A., Burnett, R. T., Thun, M. J., Calle, E. E., Krewski, D., Ito, K., & Thurston, G. D. J. J. (2002). Lung cancer, cardiopulmonary mortality, and long-term exposure to fine particulate air pollution. *287*(9), 1132-1141.

Pope III, C. A., Dockery, D. W. J. J. o. t. a., & association, w. m. (2006). Health effects of fine particulate air pollution: lines that connect. *56*(6), 709-742.

Pope III, C. A., Ezzati, M., & Dockery, D. W. J. N. E. J. o. M. (2009). Fine-particulate air pollution and life expectancy in the United States. *360*(4), 376-386.

Premuda, M., Petritoli, A., Masieri, S., Palazzi, E., Kostadinov, I., Bortoli, D., . . . Giovanelli, G. J. A. e. (2013). A study of O3 and NO2 vertical structure in a coastal wooded zone near a metropolitan area, by means of DOAS measurements. *71*, 104-114.

Richter, A., Burrows, J. P., Nüß, H., Granier, C., & Niemeier, U. J. N. (2005). Increase in tropospheric nitrogen dioxide over China observed from space. *437*(7055), 129.

Riess, J. J. U. E. P. A., Office of Air Quality Planning, & Standards. (1998). Nox: how nitrogen oxides affect the way we live and breathe. 2.

Robinson, J. K., Bollinger, M. J., & Birks, J. W. J. A. c. (1999). Luminol/H2O2 chemiluminescence detector for the analysis of nitric oxide in exhaled breath. *71*(22), 5131-5136.

Roble, R. G. J. T. U. M., Experiment, L. T. A. R. o., & Theory, G. M. S. (1995). Energetics of the mesosphere and thermosphere. *87*, 1-21.

Rothman, L. S. J. J. o. Q. S., & Transfer, R. (2010). The evolution and impact of the HITRAN molecular spectroscopic database. *111*(11), 1565-1567.

Salonen, H., Salthammer, T., & Morawska, L. J. E. i. (2019). Human exposure to NO2 in school and office indoor environments. *130*, 104887.

Schecter, A., Birnbaum, L., Ryan, J. J., & Constable, J. D. J. E. r. (2006). Dioxins: an overview. *101*(3), 419-428.

Seangkiatiyuth, K., Surapipith, V., Tantrakarnapa, K., & Lothongkum, A. W. J. J. o. E. S. (2011). Application of the AERMOD modeling system for environmental impact assessment of NO2 emissions from a cement complex. *23*(6), 931-940.

Seaton, A., Godden, D., MacNee, W., & Donaldson, K. J. T. l. (1995). Particulate air pollution and acute health effects. *345*(8943), 176-178.

Serdyuchenko, A., Gorshelev, V., Weber, M., Chehade, W., & Burrows, J. J. A. M. T. (2014). High spectral resolution ozone absorption cross-sections–Part 2: Temperature dependence. *7*(2), 625-636.

Shabbir, Y., Khokhar, M. F., Shaiganfar, R., & Wagner, T. J. J. o. E. S. (2016). Spatial variance and assessment of nitrogen dioxide pollution in major cities of Pakistan along N5-Highway. *43*, 4-14.

Shaiganfar, R., Beirle, S., Petetin, H., Zhang, Q., Beekmann, M., & Wagner, T. J. A. M. T. (2015). New concepts for the comparison of tropospheric NO 2 column densities derived from car-MAX-DOAS observations, OMI satellite observations and the regional model CHIMERE during two MEGAPOLI campaigns in Paris 2009/10. *8*(7), 2827-2852.

Takashima, H., Irie, H., Kanaya, Y., & Akimoto, H. J. A. e. (2011). Enhanced NO2 at Okinawa Island, Japan caused by rapid air-mass transport from China as observed by MAX-DOAS. *45*(15), 2593-2597.

Thalman, R., & Volkamer, R. J. P. c. c. p. (2013). Temperature dependent absorption cross-sections of O 2–O 2 collision pairs between 340 and 630 nm and at atmospherically relevant pressure. *15*(37), 15371-15381.

Theys, N., Roozendael, M. V., Hendrick, F., Fayt, C., Hermans, C., Baray, J.-L., . . . Physics. (2007). Retrieval of stratospheric and tropospheric BrO columns from multi-axis DOAS measurements at Reunion Island (21 S, 56 E). *7*(18), 4733-4749.

Tian, X., Xie, P., Xu, J., Li, A., Wang, Y., Qin, M., & Hu, Z. J. J. o. E. S. (2018). Long-term observations of tropospheric NO2, SO2 and HCHO by MAX-DOAS in Yangtze River Delta area, China. *71*, 207-221.

Van Der A, R., Eskes, H., Boersma, K., Van Noije, T., Van Roozendael, M., De Smedt, I., . . . Meijer, E. J. J. o. G. R. A. (2008). Trends, seasonal variability and dominant NOx source derived from a ten year record of NO2 measured from space. *113*(D4).

Van Der A, R., Peters, D., Eskes, H., Boersma, K., Van Roozendael, M., De Smedt, I., & Kelder, H. J. J. o. G. R. A. (2006). Detection of the trend and seasonal variation in tropospheric NO2 over China. *111*(D12).

Vandaele, A. C., Hermans, C., Simon, P. C., Van Roozendael, M., Guilmot, J. M., Carleer, M., & Colin, R. J. J. o. a. c. (1996). Fourier transform measurement of NO 2 absorption cross-section in the visible range at room temperature. *25*(3), 289-305.

Vlemmix, T., Hendrick, F., Pinardi, G., Smedt, I. D., Fayt, C., Hermans, C., . . . Roozendael, M. V. J. A. M. T. (2015). MAX-DOAS observations of aerosols, formaldehyde and nitrogen dioxide in the Beijing area: comparison of two profile retrieval approaches. *8*(2), 941-963.

Vlemmix, T., Piters, A., Stammes, P., Wang, P., & Levelt, P. J. A. M. T. (2010). Retrieval of tropospheric NO 2 using the MAX-DOAS method combined with relative intensity measurements for aerosol correction. *3*(5), 1287-1305.

Wagner, T., Beirle, S., Brauers, T., Deutschmann, T., Frieß, U., Hak, C., . . . Li, X. J. A. M. T. (2011). Inversion of tropospheric profiles of aerosol extinction and HCHO and NO 2 mixing ratios from MAX-DOAS observations in Milano during the summer of 2003 and comparison with independent data sets. *4*(12), 2685-2715.

Wagner, T., Dix, B. v., Friedeburg, C. v., Frieß, U., Sanghavi, S., Sinreich, R., & Platt, U. J. J. o. G. R. A. (2004). MAX-DOAS O4 measurements: A new technique to derive information on atmospheric aerosols—Principles and information content. *109*(D22).

Wagner, T., Ibrahim, O., Shaiganfar, R., & Platt, U. J. A. m. t. (2010). Mobile MAX-DOAS observations of tropospheric trace gases. *3*(1), 129-140.

Wang, S., Zhou, B., Wang, Z., Yang, S., Hao, N., Valks, P., . . . Chen, L. J. J. o. G. R. A. (2012). Remote sensing of NO2 emission from the central urban area of Shanghai (China) using the mobile DOAS technique. *117*(D13).

Wang, Y., Lampel, J., Xie, P., Beirle, S., Li, A., Wu, D., & Wagner, T. (2017). Ground-based MAX-DOAS observations of tropospheric aerosols, NO2, SO2 and HCHO in Wuxi, China, from 2011 to 2014.

Wittrock, F., Oetjen, H., Richter, A., Fietkau, S., Medeke, T., Rozanov, A., . . . Physics. (2004). MAX-DOAS measurements of atmospheric trace gases in Ny-Ålesund-Radiative transfer studies and their application. *4*(4), 955-966.

Zafar, L., Ahmad, S., Syed, W., & Ali, S. J. S. I. (2012). Temporal variations in nitrogen dioxide concentration due to vehicular emissions in Islamabad capital territory (ICT) & Rawalpindi. *24*(3), 265-268.

Zhang, Q., Shen, Z., Cao, J., Zhang, R., Zhang, L., Huang, R.-J., . . . Xu, H. J. A. e. (2015). Variations in PM2. 5, TSP, BC, and trace gases (NO2, SO2, and O3) between haze and non-haze episodes in winter over Xi'an, China. *112*, 64-71.